

Formation of highly oxygenated organic molecules from aromatic compounds.

Ugo Molteni¹, Federico Bianchi⁺², Felix Klein¹, Imad El Haddad¹, Carla Frege¹, Michel J. Rossi¹, Josef Dommen¹, Urs Baltensperger^{1,*}

5 ¹Laboratory of Atmospheric Chemistry, Paul Scherrer Institute, CH-5232 Villigen, Switzerland

²Department of Physics, University of Helsinki, 00014 Helsinki, Finland

Correspondence to: Urs Baltensperger (urs.baltensperger@psi.ch)

Abstract

10 Anthropogenic volatile organic compounds (AVOC) often dominate the urban atmosphere and consist to a large degree of aromatic hydrocarbons (ArHC), such as benzene, toluene, xylenes, and trimethylbenzenes, e.g. from handling and combustion of fuels. These compounds are important precursors for the formation of secondary organic aerosol. Despite their recognized importance as atmospheric reactants, the formation of highly oxygenated molecules (HOMs) in the gas phase leading to (extremely) low volatility compounds has not been studied in the past. Here we show that oxidation of aromatics with OH leads to a subsequent autoxidation chain reaction forming HOMs with an O:C ratio of up to 1.09. This is exemplified for five single-ring ArHC (benzene, toluene, o-/m-/p-xylene, mesitylene (1,3,5-trimethylbenzene) and ethylbenzene), as well as two conjugated polycyclic ArHC (naphthalene and biphenyl). ~~We present the identified compounds, differences in the observed oxidation patterns and discuss mechanistic pathways. We report the elemental composition of the HOMs and show the differences in the oxidation patterns of these ArHCs. A potential pathway for the~~
15 ~~formation of these HOMs from aromatics is presented and discussed.~~ We hypothesize that AVOC may contribute substantially to new particle formation events that have been detected in urban areas.
20

1 Introduction

Volatile organic compounds (VOCs) from biogenic and anthropogenic sources are the precursors of atmospheric oxidation products in the gas and particle phase. While global biogenic VOC (BVOC) emissions are a factor of 10 higher than the emissions of anthropogenic VOCs (AVOCs), the latter often dominate in the urban atmosphere (Atkinson and Arey, 2003). It was shown recently that atmospheric oxidation products of BVOCs, such as the monoterpene alpha-pinene, include highly oxygenated molecules (HOMs) through an autoxidation mechanism (Crouse et al., 2012, 2013; Ehn et al., 2014). The first step is a reaction of either OH free radicals or ozone with the VOC. After addition of O₂ to the carbon-centered radical site the RO₂· radical can isomerize by intra-molecular hydrogen abstraction to form a new carbon-centered radical (QOOH)
30 (Crouse et al., 2012, 2013; Ehn et al., 2014). Further O₂-addition/isomerization sequences result in HOMs bearing several

hydroperoxy groups. This autoxidation mechanism is supported by various experimental studies which used biogenic precursors, i.e. monoterpenes, sesquiterpenes, isoprene, and structural surrogates of these and computer simulations (Berndt et al., 2015; Jokinen et al., 2014, 2015; Kurtén et al., 2015; Mentel et al., 2015; Praplan et al., 2015; Richters et al., 2016; Rissanen et al., 2014, 2015). HOMs of those compounds were found to initiate new particle formation and substantially contribute to early particle growth, which is important for the survival of newly formed particles and their ability to form cloud condensation nuclei, CCN (Bianchi et al., 2016; Kirkby et al., 2016; Tröstl et al., 2016). ~~CCN can impact climate via their influence on cloud properties nowadays and in the pre-industrial period~~ CCN can impact climate via their influence on cloud properties; this changes the radiation balance nowadays and did even more so in the pre-industrial period (Carslaw et al., 2013; Gordon et al., 2016).

AVOCs are comprised of a high fraction of aromatic hydrocarbons (ArHC), such as benzene, toluene, xylenes, and trimethylbenzenes, which are released from handling and combustion of fuels (Atkinson and Arey, 2003), and are important precursors for the formation of secondary organic aerosol (SOA) (Bruns et al., 2016; Li et al., 2016; Metzger et al., 2010). The OH radical is the preponderant atmospheric oxidant for ArHC except for phenols or substituted ArHC with non-aromatic double bonds where ozone and the NO₃ radical play a relevant role (Calvert et al., 2002). The addition of the OH radical to the aromatic ring results in the formation of a hydroxycyclohexadienyl-type radical (Bohn, 2001; Molina et al., 1999). Despite the fact that ArHC·OH adducts under atmospheric conditions react with O₂ to yield peroxy radicals (Calvert et al., 2002; Glowacki and Pilling, 2010; Suh et al., 2003) ~~and the recognized importance of ArHC in the photochemical production of ozone and SOA, it is not known if ArHC oxidation also yields HOMs (Birdsall and Elrod, 2011; Li and Wang, 2014; Pan and Wang, 2014; Wang et al., 2013; Zhang et al., 2012). This could be linked to the fact that the relevant processes were neither accessible by flash photolysis nor by smog chamber experiments (Glowacki and Pilling, 2010) and instrument limitations. In many studies no carbon balance could be reached and generally only about 50% of the carbon reacted was identified as products it is not known if ArHC oxidation also yields HOMs. No carbon balance could be reached so far and generally only about 50% of the carbon reacted was identified as products~~ (Calvert et al., 2002). When aromaticity is ~~destroyed lost~~ by OH-addition, non-aromatic double bonds are formed, ~~thus representing highly reactive products, which is a peculiar behaviour not observed in other classes of VOC~~ representing highly reactive products to more oxidants, which is a peculiar behaviour not observed in other classes of VOC (Calvert et al., 2002). This behaviour makes the investigation of ArHC oxidation more complex.

Here we show the formation of HOMs from ArHC upon reaction with OH radicals. We present product distributions of HOMs in terms of molecular masses and molecular formulas for a series of aromatic precursors based on measurements with a nitrate chemical ionization atmospheric pressure interface time of flight mass spectrometer (CI-API-TOF) ~~Here we present product distributions in terms of molecular masses for ArHC HOMs upon reaction of aromatic compounds with OH radicals, based on measurements with a nitrate chemical ionization atmospheric pressure interface time of flight mass spectrometer (CI-API-TOF)~~ (Ehn et al., 2014; Jokinen et al., 2012; Kürten et al., 2011). ~~Potential pathways and a possible mechanism for~~

65 ~~the formation of HOMs from aromatic compounds are discussed. A potential pathway along with a possible mechanism for~~
the formation of HOMs from aromatic compounds is discussed.

2 Experimental section

2.1 Flow tube

70 Five single-ring ArHCs: benzene (Merck), toluene (VWR Chemicals), a mixture of o-/m-/p-xylene isomers (Merck), mesitylene (1,3,5-trimethylbenzene) (Fluka), ethylbenzene (Fluka), as well as two polycyclic ArHCs naphthalene (Fluka) and biphenyl (Sigma-Aldrich) were investigated in a flow tube (Table 1). The experimental set-up is shown in Figure 1. Zero air from a pure air generator (Aadco Instruments, Inc., Cleves OH, USA) was used. A 104-cm long Pyrex glass tube of 7.4 cm diameter described previously (Pratte and Rossi, 2006) was used as a flow tube. Vapours of the aromatic compounds were generated from a glass vial, and collected by a stream of zero air (1.1 L min⁻¹) via a glass capillary for liquid compounds (and from a flask flushed with the same stream of zero air for solid compounds). To generate OH free radicals, zero air (7 L min⁻¹) was passed through a Nafion humidifier (Perma Pure) fed with ultra-pure water, and was then irradiated by an excimer lamp at 172 nm (7.2 eV) (Kogelschatz, 1990, 2012; Salvermoser et al., 2008). The Xe excimer lamp has a coaxial geometry and consists of a tubular quartz cell which surrounds a quartz flow tube (outer diameter 10 mm) which is used as OH radical generator. Previous works (Bartels-Rausch et al., 2011) used this set up for HO₂ radical generation. Subsequently, the air stream with the OH free radicals was combined at an angle of 90 degrees with the reagent flow containing the aromatic vapours before entering the flow tube, initiating the oxidation reaction. This experimental set-up avoids any potential bias due to exposure of ArHC vapours to UV radiation (Jain et al., 2012; Peng et al., 2016). This mixture (total 8.1 L min⁻¹) was injected into a laminar sheath flow of 6.7 L min⁻¹ zero air at the inlet of the flow tube. The residence time in the flow tube was 20 sec. All experiments were performed at 25° C. A description of the chemical reactions involved in the excimer lamp OH radical production and a flow tube kinetic model for the mesitylene oxidation are given in
85 Appendix C.

2.2 Instruments

90 The concentration of the ArHC precursors and D9-butanol as an OH tracer was measured at the exit of the flow tube with a proton-transfer-reaction time of flight mass spectrometer (PTR-TOF-MS) (Jordan et al., 2009) when the excimer lamp to generate OH free radicals was switched off and on. A nitrate chemical ionization atmospheric pressure interface time of flight mass spectrometer (CI-APi-TOF) (Ehn et al., 2014; Jokinen et al., 2012; Kürten et al., 2011) measured the chemical composition of the HOMs that were formed via OH free radical oxidation of the aromatics. HOMs were detected either through acid-base reaction or adduct formation with a nitrate ion according to the scheme:



95 Trifluoroacetic acid (monomer and dimer) was detected as major contaminant in the CI-API-TOF spectra. We identified the Nafion humidifier membrane as the source of fluorinated organic compounds.

~~The OH free radical concentration was estimated from two separate experiments using D9-butanol following the method of Barmet et al. (2012). From the D9-butanol signal with excimer lamp on and off we obtained an average OH concentration of $(1.9 \pm 0.4) \cdot 10^8$ molecules cm^{-3} . HOMs yields are calculated as the ratio of HOMs measured to ArHC reacted. HOMs were quantified using the calibration factor for sulfuric acid and assuming the same charging efficiency for HOMs (Ehn et al., 2014; Kirkby et al., 2016). From the decrease of the precursor concentration (lights off versus lights on) we determined an average OH concentration. From the experiments with D9-butanol, toluene, mesitylene and biphenyl an average OH concentration of $2 \cdot 10^8$ OH cm^{-3} was obtained. Assuming the same OH production of the lamp in all experiments ArHC reacted was calculated from the OH radical exposure using the reaction rate coefficients at 25°C. Ozone, produced in the excimer irradiated region as a side product of OH generation, was measured to be about 140 ppbv at the exit of the flow tube and is therefore not expected to play a significant role in the oxidation of ArHC in flow tube experiments.~~

100
105

3 Results and discussion

3.1 Comparison of HOMs from different ArHC

The oxidation products of the OH reaction with each of the five single-ring and two polycyclic ArHCs were measured at the exit of the tube using the CI-API-TOF. Table 1 lists the initial concentration and the reaction rate constant of them with the OH radical. ~~the reacted fraction (%), the HOMs concentration and the HOMs yield (%) calculated based on the reacted precursor, and ozone, respectively.~~ All investigated compounds yielded HOMs in a range between 0.31 and 1.4 % of the reacted ArHC. They were detected either as adducts with a nitrate ion (NO_3^-) or as deprotonated ions. Appendix A presents HOMs peak lists for all the ArHC compounds: for each compound we report the first n peaks that sum up to 80% of the total detected signal of HOMs. Figure 2 displays the mass spectra obtained from the monocyclic aromatics. In the mass-to-charge (m/z) range 130 – 365 thomson (Th; 1 Th = 1 Da e^{-1} , where e is the elementary charge), the oxidation products contain the carbon skeleton of the precursor (monomer region), while in the m/z range 285 – 540 Th the number of carbon atoms is doubled (dimer region). The lower end of the peak sequence (which for the benzene experiment corresponds to the oxidation product with formula $\text{C}_6\text{H}_6\text{O}_5(\text{NO}_3^-)$) is shifted by differences of 14 Th (CH_2) each from benzene via toluene and xylene/ethylbenzene to mesitylene due to the additional ~~methyl/ethyl~~substituent groups. In general, a series of peaks with a mass difference of two oxygen atoms can be seen in the monomer as well as the dimer region. At each oxygen addition a few peaks are observed because oxidation compounds with the same carbon and oxygen number but different hydrogen number were observed. These peaks can be attributed to closed shell or radical compounds based on the number of hydrogen (even or odd).

110
115
120

125 HOMs from naphthalene and biphenyl are presented in Figure 3. Monomers, dimers, trimers, and tetramers are observed, and even pentamers for biphenyl. While some of the dimers may have been formed by $\text{RO}_2\cdot - \text{RO}_2\cdot$ reactions, most of the higher n -mers are probably bonded by ~~Van der Waalsintermolecular~~ interactions, similar to ~~the mechanism for~~ biogenic HOMs (~~Kirkby et al., 2016; Tröstl et al., 2016~~) (Donahue et al., 2013). Clusters with $m/z \geq 800$ Th might already be detected ~~as particles by particle counters~~ with a mobility diameter $d \geq 1.5$ nm (Kulmala et al., 2013).

130 In Table 2 we summarize the general features of the peak distribution of monomers, dimers and n -mers, as well their O:C ratios. The values given in the table cannot be considered to be absolute values, since we do not know the transmission function of the mass spectrometer. Thus, the dimer/monomer ratio might be different. ~~However, since the mass-dependent ion transmission efficiency is rather smooth the given values may faithfully represent the relative product distribution of the different aromatic compounds.~~ However, the given values may be a good proxy of the relative behaviour of the product distribution of the different aromatic compounds. Most of the identified peaks (77-94%) were detected as adduct with NO_3^- .

135 The integrated signal intensity in the monomer region makes up 61 to 80% of the total detected ArHC products signal for the monocyclic ArHCs and 34-52% for the double-ring compounds. A further analysis of HOMs from monocyclic ArHC shows an increase in the dimer fraction which coincides with an increase in the methyl/ethyl substituents as follows: benzene (20%), toluene (29%), ethylbenzene (31%), xylene (35%), mesitylene (39%). ~~If we assume that the HO_2 concentration is similar, then the branching ratio of $\text{RO}_2\cdot + \text{RO}_2\cdot$ to dimer compared to the other reaction channels is higher for the more substituted aromatics. This indicates that the branching ratio of $\text{RO}_2\cdot + \text{RO}_2\cdot$ to dimer (R3c) compared to the other reaction channels (R3a,b) is higher for the more substituted aromatics. This is based on the assumption that the lamp produces similar concentrations of OH and HO_2 radicals and that the reaction rate coefficients $k(\text{RO}_2\cdot + \text{HO}_2\cdot)$ (R4a) are similar for all $\text{RO}_2\cdot$.~~

140 Monomers as well as dimers are highly oxygenated, even though the molecular oxygen-to-carbon (O:C) ratio is 20-30% higher for the monomers compared to the dimers. Single-ring ArHC monomers have on average an O:C ratio of 0.94 (0.50 for the double-ring ArHC) while ~~monocyclic ArHC dimers~~ ~~dimers that were generated from monocyclic ArHC~~ have on average an O:C ratio of 0.67 (0.32 for the double-ring ArHC). This may be due to the dimer formation mechanism itself, which is thought to be the formation of a peroxide C-O-O-C bond which involves elimination of molecular oxygen (~~Kirkby et al., 2016; Wallington et al., 1992~~) (Mentel et al., 2015; Wallington et al., 1992). Additionally, more oxygenated radicals have a higher probability to undergo an ~~unimolecular termination~~ ~~auto-termination~~ ~~radical reaction~~ compared to a radical-radical recombination ($\text{RO}_2\cdot + \text{RO}_2\cdot$ or $\text{RO}_2\cdot + \text{HO}_2\cdot$). ~~More oxygen atoms imply more peroxy functional groups and therefore a higher probability of a hydrogen abstraction in geminal position of a peroxide which results in an OH radical loss and a carbonyl group formation. Therefore, the fraction of dimer formation should decrease with higher oxygen content. Furthermore, less oxygenated products are not quantitatively detected by the CI-API-TOF. Furthermore, we assume that less oxygenated radicals, although not quantitatively detected by the CI-API-TOF~~ (Berndt et al., 2015; Hyttinen et al., 2015) ~~but such radicals are nevertheless taking part in the dimer formation.~~, ~~will nevertheless participate in the dimer formation.~~

145

150

155 Substantially lower O:C ratios are found for naphthalene and biphenyl, whereby the trend between the monomers and the

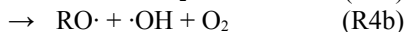
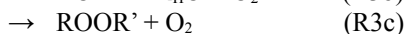
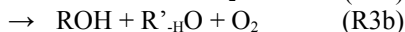
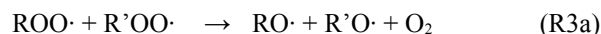
dimers and higher order clusters is the same as for the single-ring ArHCs. The lower O:C ratio is probably owing to the fact that the second aromatic ring remains and does not allow for extensive autoxidation.

Figure 4 shows the contribution of the most abundant identified HOMs to 80% of the total signal. The chemical composition of the observed monomers, dimers and radicals for each precursor is presented in Appendix B (Figure B-1 to Figure B-7). It is seen that in the series benzene, toluene, xylene, mesitylene the number of HOMs needed to sum up 80% of the total signal decreases (except for ethylbenzene). The increasing number of methyl groups appears to influence the oxidation pathways and leads to less HOM products. Ethylbenzene shows the highest number of HOMs. These also include monomers with 7 carbon atoms as well as dimers with an unexpectedly low number of hydrogen atoms (20 instead of 22) (Figure B – 3). This could indicate the occurrence of different pathways due to the ethyl group, a chemistry less bounded to the aromatic ring which implies an initial hydrogen abstraction step by the OH radical. Together with ethylbenzene also benzene and naphthalene, the two not substituted ArHC tested, present dimers with an unexpected low hydrogen number (12 instead of 14 and 16 instead of 18). Biphenyl also shows an unexpectedly low number of hydrogen atoms for some of the HOM monomers detected. This feature, highlighted in the four above-mentioned compounds, turns out to be a minority in terms of peaks detected and relative peak intensity.

3.2 ArHC HOMs formation mechanism

A generalized mechanism that may explain the formation of these highly oxygenated compounds from ArHCs by OH addition is exemplified for mesitylene in Figure 5. This mechanism is also applicable to the other ArHCs tested. An OH free radical attack on alkyl-substituted arenes is thought to either abstract a hydrogen atom from an sp^3 hybridized carbon, or to add to the aromatic ring. Starting from a generic aromatic compound with formula C_xH_y , hydrogen abstraction results in a C_xH_{y-1} radical while OH addition results in a radical with the formula $C_xH_{y+1}O_1$. If we allow both initial intermediate products to proceed via autoxidation by formal addition of O_2 , we expect radicals with the composition $C_xH_{y-1}O_{ze}$ (initial hydrogen abstraction) and $C_xH_{y+1}O_{zo}$ (initial OH addition) to be formed, where z denotes the any number of oxygen atoms, even number (ze) in the former case and odd number (zo) in the latter case. This addition of molecular O_2 increases the mass of the compounds by 32 Da resulting in the propagation of a radical with an odd number of oxygen atoms. This can be seen by m/z shifts of 32 Th in the mass spectra. For the ArHCs tested we do not observe radicals with the formula $C_xH_{y-1}O_{ze}$, owing to the fact that hydrogen abstraction is a minor pathway (with e.g. a branching ratio of 7% for toluene according to the Master Chemical Mechanism MCM 3.3.1 (Jenkin et al., 2003), which yields products like benzaldehyde and benzyl alcohol). For mesitylene (Figure 5), the OH-adduct and the first $RO_2\cdot$ radical ($HO-C_xH_yOO\cdot$) cannot be detected with the nitrate CI-API-TOF (Hyttinen et al., 2015) and are reported in grey in Figure 5. More highly oxygenated $RO_2\cdot$ radicals with the formula $C_9H_{13}O_{5-11}$ were however found, with the highest intensity for $C_9H_{13}O_7$ (3% of the sum of the identified HOMs). In addition to radicals with an odd oxygen number, radicals with an even oxygen number of molecular formula $C_xH_{y+1}O_{ze}$ were observed (Figure 5). These radicals are likely produced via $RO_2\cdot + RO_2\cdot$ (or $RO_2\cdot + HO_2\cdot$), involving the formation of an alkoxy radical

190 intermediate (Lightfoot et al., 1992; Mentel et al., 2015; Orlando and Tyndall, 2012; Vereecken and Peeters, 2009) according to:



195 These alkoxy radicals (R3a and R4b) may isomerize to an alcohol by internal H-abstraction forming a carbon centred radical, which can again uptake an oxygen atom molecule and follow the autoxidation route. The peroxy radicals of this reaction channel have the formula $\text{C}_x\text{H}_{y+1}\text{O}_z$ (see Fig.5). Besides the formation of alkoxy radicals recombination can also lead to a carbonyl and alcohol species (R3b) with the formulae $\text{C}_x\text{H}_y\text{O}_z$ and $\text{C}_x\text{H}_{y+2}\text{O}_z$. ~~The discrepancy between the intensity of the peaks with formula $\text{C}_x\text{H}_y\text{O}_z$ and the peaks with formula $\text{C}_x\text{H}_{y+2}\text{O}_z$ can be ascribed to the presence of compounds resulting from the recombination of $\text{RO}_2\cdot$ with $\text{HO}_2\cdot$ in the latter class (R4a). The much higher intensity of the peaks with~~
200 ~~formula $\text{C}_x\text{H}_{y+2}\text{O}_z$ compared to those with the composition $\text{C}_x\text{H}_y\text{O}_z$ can be ascribed to a high contribution from the recombination of $\text{RO}_2\cdot$ with $\text{HO}_2\cdot$ (R4a). This is due to the high $\text{HO}_2\cdot$ concentration in our experiments since $\text{HO}_2\cdot$ is also formed in the OH radical source.~~ The formation of ROOR (R3c) corresponds to $\text{C}_{2x}\text{H}_{2y+2}\text{O}_z$ dimer formation with z being even or odd, depending on the combination of the reacting peroxy radicals. We also detected free radicals and closed-shell molecules with an unexpectedly high number of hydrogen atoms, with the formulae $\text{C}_x\text{H}_{y+(3,5)}\text{O}_z$ and $\text{C}_x\text{H}_{y+(4,6)}\text{O}_z$, respectively.
205 For mesitylene (Fig. 5), radicals with the formula $\text{C}_9\text{H}_{15}\text{O}_{7-11}$ were identified, with the highest signals found for $\text{C}_9\text{H}_{15}\text{O}_7$ (1%), and $\text{C}_9\text{H}_{15}\text{O}_8$ (2%). These compounds are likely formed by a second OH addition as discussed further below. Monomer closed-shell molecules were detected as $\text{C}_9\text{H}_{12}\text{O}_{5-11}$ (4%), $\text{C}_9\text{H}_{14}\text{O}_{4-11}$ (25%), and $\text{C}_9\text{H}_{16}\text{O}_{5-10}$ (12%). We assume that the $\text{C}_9\text{H}_{12}\text{O}_{5-11}$ molecules derive from the first radical generation ($\text{C}_9\text{H}_{13}\text{O}_{5-11}$) and the $\text{C}_9\text{H}_{16}\text{O}_{5-10}$ molecules from a second OH attack ($\text{C}_9\text{H}_{15}\text{O}_{7-11}$). The $\text{C}_9\text{H}_{14}\text{O}_{4-11}$ molecules may be produced from either the first or the second OH attack. However
210 further investigation is required to test these hypotheses. We also want to point out that the relative signal intensities may be biased by the nitrate clustering properties and do not necessarily reflect the actual distribution of compounds. ~~Similarly, the compounds with a lower than expected H-atom number could have been formed by a H-abstraction from first generation products with formula $\text{C}_x\text{H}_y\text{O}_z$. Similarly, the compounds with an H-atom number lower than the ArHC precursor could have been formed by an H-abstraction from first generation products with formula $\text{C}_x\text{H}_y\text{O}_z$.~~
215 The recombination of two peroxy radicals may lead to a covalently-bound peroxy-bridged dimer. We observed three classes of such products (Figure 5): i) from the recombination of two first-generation radicals (13 hydrogen atoms each) with the molecular formula $\text{C}_{18}\text{H}_{26}\text{O}_{8-13}$ (30% of the total intensity), ii) from the recombination of a first generation radical with a second generation radical (13 + 15 hydrogen atoms) with formula $\text{C}_{18}\text{H}_{28}\text{O}_{9-12}$ (3% of the total signal), and iii) from the recombination of two radicals from the second generation (15 + 15 hydrogen atoms), where only one compound was
220 identified ($\text{C}_{18}\text{H}_{30}\text{O}_{11}$, 1%).

Some identified monomer and dimer peaks belong to oxygenated molecules with less carbon atoms than the respective precursor. This is likely the result of a fragmentation process. HOMs with less C atoms than the parent molecule have also been previously described from terpene precursors via CO elimination~~HOMs with less C atoms than the parent molecule have also been previously described from terpene precursors via CO elimination~~ (Rissanen et al., 2014, 2015). Here, the aromatics show mostly also a loss of H-atoms when fragmenting. This indicates that a methyl group can be lost after oxidation to an alkoxy radical as formaldehyde or a carbon fragment can be lost after ring cleavage. The aromatics show mostly much less H-atoms than the terpenes after fragmentation. This indicates that a methyl group is lost, e.g. as formaldehyde. As mentioned above, we hypothesize that the $C_xH_{y+(3,5)}O_z$ radicals and $C_xH_{y+(4,6)}O_z$ molecules may have formed by multiple OH attacks in our reactor. This is possible when the second OH attacks a product molecule that contains two hydrogen atoms more than the parent molecule. To allow for the addition of a second OH free radical these first generation closed-shell molecules must still contain a double bond in their structure. ~~A third OH attack is observed only for some compounds; the mechanism will likely proceed in a similar way~~A third OH attack is observed only for some compounds: benzene, ethylbenzene, xylene, naphthalene and biphenyl; the contribution of these HOMs to the total of the detected signals is always extremely low. The mechanism will likely proceed in a similar way.

235 An explicit mechanism after OH addition for a possible pathway of the aromatic autoxidation is suggested in Figure 6 for up to seven oxygen atoms. ~~Compared to aliphatic compounds, for which the autoxidation mechanism proceeds by hydrogen abstraction and formation of a hydroperoxyalkyl radical that reacts with molecular oxygen, aromatic compounds – once their aromaticity is lost – can form a conjugated radical in the allylic position for a subsequent molecular oxygen attack and peroxy radical formation~~After addition of OH and loss of aromaticity an oxygen molecule can be added forming a peroxy radical. It has been established that the latter can cyclize producing a second stabilized allylic radical with an endocyclic O_2 bridge (Baltaretu et al., 2009; Birdsall and Elrod, 2011; Pan and Wang, 2014). On this oxygen bridged bicyclic radical further oxygen addition and cyclization might occur up to a peroxy radical with seven oxygen atoms ($C_9H_{13}O_7$), which is the species detected at relatively high intensity (3.5%). This process can continue up to seven oxygen atoms ($C_9H_{13}O_7$), which is the species detected at relatively high intensity (3.5%). The peroxy radical then can either abstract a hydrogen atom, when possible, or attack the double bond producing a second stabilized allylic radical forming an endocyclic O_2 bridge. This mechanism varies among the ArHC tested. Aromatics with a lower number of methyl/ethyl substituents seem to form radicals with a higher number of oxygen (i.e., up to 9-11 atoms, Appendix B). However, it appears that a single ring ArHC can host up to a maximum of 11 oxygen atoms and a ring opening step seems to be a requirement to reach such a high O:C ratio. In Figure 6 we hypothesize possible branching channels where this may happen. A peroxy radical recombination can form an alkoxy radical which can decompose by a C-C bond cleavage yielding a carbonyl group and a carbon centred radical. Such a ring opening step was already proposed for α -pinene to explain the high O:C ratio (Kurtén et al., 2015). Termination reactions of those alkoxy radicals can also form molecules containing still double bonds which can further react with OH radicals leading to compounds with four hydrogen atoms more than the precursor. As mentioned above naphthalene and biphenyl, despite the polycyclic skeleton, do not show a radically different behaviour compared to the single-ring

255 ArHCs. The maximum number of oxygen atoms that their monomer HOMs can host is 10 for naphthalene and 11 for biphenyl. Biphenyl seems to compare with its single ring analogue benzene. $C_6H_8O_5$ and $C_{12}H_{12}O_5$ are the strongest peaks indicating that the oxidation of one benzene ring in biphenyl proceeds in a similar way. Similarly, the strongest dimer is $C_{12}H_{14}O_8$ for benzene and $C_{24}H_{22}O_8$ for biphenyl, respectively. Compounds with extra-high H-atoms are more frequently found for biphenyl, which is expected as there is a second reactive aromatic ring remaining after (auto)-oxidation of the first one. Thus, a second OH attack is easily possible. Naphthalene seems to take up less oxygen than the other compounds, showing the maximum signal intensity at 4-5 oxygen atoms for monomers and only 4-6 for dimers. This may indicate that not both rings can easily be autoxidized in one step. It is also interesting to note that compounds from a second OH attack do not show a strong increase of the oxygen content, neither for the single nor for the double ring ArHCs.

4 Conclusions and atmospheric implications

265 All tested compounds yielded HOMs and we conclude that this is a common feature of aromatic compounds. Similar to the oxidation process that yields HOMs from terpenes the oxidation process of ArHC yields highly oxygenated compounds containing the carbon skeleton of the precursor (monomers) as well as twice as many carbons (dimers). It is known from previous studies that ArHC are able to add molecular oxygen to the molecule after OH addition forming an oxygen-bridged bicyclic radical. Our measurements of highly oxygenated compounds up to eleven oxygen atoms in a monomer reveal that an autoxidation radical chain reaction occurs by adding several more oxygens to the initially formed radical. The autoxidation radical chain reaction is thought to proceed via intra-molecular abstraction of a hydrogen atom from an acidic C-H bond by a peroxy radical and the consequent formation of a hydroperoxy functional group and a carbon centered radical that can take up an oxygen molecule from the surrounding and eventually repeat the whole process n times (here called Type I autoxidation). In the case of aromatic compounds, when the aromaticity is destroyed, Type II autoxidation may happen by further addition of oxygen to the allylic resonance-stabilized radical followed by an attack of the peroxy group to the internal double bonds forming an oxygen bridge. This can proceed up to a peroxy radical of 7 oxygen. We speculate that Type II autoxidation might also occur in organic molecules with two double bonds like isoprene and limonene. This may happen by further addition of oxygen to the allylic resonance-stabilized radical and formation of oxygen bridges up to a peroxy radical of 7 oxygen. The autoxidation chain may also proceed after a ring opening intermediate step. Even though the autoxidation of ArHCs will lead to different chemical compounds compared to HOMs from terpenes we expect similar chemical and physical characteristics such as functional groups ~~or~~and volatility. In both cases extremely low volatility highly oxygenated dimer species are formed, which may play an important role in new particle formation.

Recent studies (Nakao et al., 2011; Schwantes et al., 2016) ~~suggest a mechanism where the initial step is the formation of the phenolic equivalent ArHC followed by additional oxidation steps yielding “polyphenolic” structures with high O:C ratio. Literature data are showing varying yields for the conversion of arenes to phenols via the OH radical addition and H elimination suggest a mechanism where the initial step is the formation of the phenolic equivalent ArHC followed by~~

290 additional oxidation steps yielding “polyphenolic” structures with high O:C ratio (up to 1.2). However literature data are showing varying yields for the conversion of arenes to phenols via the OH radical addition and H elimination. According to MCM 3.3.1 (Jenkin et al., 2003) benzene and toluene have quite high phenol yields (approximately 50 and 20 %, respectively) while mesitylene shows a rather small yield (4%). This fact should be reflected in the final HOMs yield with alkyl substituted ArHCs being less effective in yielding HOMs. However in our experiments we did not detect such a difference in the HOMs yields linked to phenol formation yields. A relevant fraction of the detected HOMs showed a hydrogen atom number higher than the precursor ArHC which cannot be explained with the presence of just polyphenolic compounds as oxidation products. benzene and toluene have quite high phenol yields (approximately 50 and 20 %, respectively) while mesitylene shows a rather small yield (4%). In our experiments we do not detect such a difference in the HOMs formation linked to phenol formation yields. We therefore believe that the formation of these ArHC HOMs is a separate oxidation process

300 Under urban conditions, in the presence of NO, the reaction of $RO_2 + NO$ will compete with the autoxidation pathway. This can lead to relatively highly oxygenated nitrates of low volatility or oxyradicals. The latter can isomerize to a carbon centred radical as under our conditions and again undergo autoxidation. Highly oxygenated organic nitrates have been recently identified in SOA (Lee et al., 2016). While this study shows that autoxidation can also occur after an OH attack of ArHC, the formation of low volatility products via this route in the presence of NO, which is typical of urban atmospheres, needs further investigation. First generation oxidation products may still contain carbon-carbon double bonds, which could also further react with ozone forming more highly oxygenated products. Since the reaction time is very short in the flow tube this reaction is negligible but could be another potential pathway in the ambient atmosphere.

305 Some of the ArHC HOMs identified here from the oxidation of ArHC correspond to the HOMs formulae identified by Some of the HOMs measured here from the oxidation of ArHC have the same composition as the HOMs formulae identified by Bianchi et al. (2016) during winter time nucleation episodes at the Jungfraujoch High Altitude Research Station.-

310 Our findings can help in explaining the missing carbon balance in ArHC oxidation experiments. Furthermore, the fact that the oxidation of aromatic compounds can rapidly form HOMs of very low volatility makes these potential contributors in nucleation and particle growth episodes observed in urban areas where these ArHC are abundant which makes ArHC a potential contributor in nucleation and particle growth episodes observed in urban areas where AVOCs are thought to play a key role. Furthermore, the fact that the oxidation of ArHC can rapidly form HOMs of very low volatility makes ArHC a potential contributor to nucleation and early particle growth during nucleation episodes observed in urban areas. (Stanier et al., 2004; Wang et al., 2015; Xiao et al., 2015; Yu et al., 2016).

Acknowledgments.

320 | We thank Prof. Dr. Markus Ammann for the laboratory equipment, ~~Dr. Kilitie~~ Dogushan Kilitie for technical support, Dr. Simone Maria Pieber and Dr. Christopher Robert Hoyle for scientific discussions and comments on the manuscript. The tofTools team is acknowledged for providing tools for mass spectrometry analysis. This work was supported by the Swiss National Science Foundation (20020_152907 / 1).

References

- Atkinson, R. and Arey, J.: Atmospheric degradation of volatile organic compounds, *Chem. Rev.*, 103(12), 4605–4638, doi:10.1021/cr0206420, 2003.
- Baltaretu, C. O., Lichtman, E. I., Hadler, A. B. and Elrod, M. J.: Primary atmospheric oxidation mechanism for toluene, *J. Phys. Chem. A*, 113(1), 221–230, doi:10.1021/jp806841t, 2009.
- Bartels-Rausch, T., Ulrich, T., Huthwelker, T. and Ammann, M.: A novel synthesis of the N-13 labeled atmospheric trace gas peroxyacetic acid, *Radiochim. Acta*, 99(5), 285–292, doi:10.1524/ract.2011.1830, 2011.
- 330 Berndt, T., Richters, S., Kaethner, R., Voigtländer, J., Stratmann, F., Sipilä, M., Kulmala, M. and Herrmann, H.: Gas-phase ozonolysis of cycloalkenes: formation of highly oxidized RO₂ radicals and their reactions with NO, NO₂, SO₂ and Other RO₂ radicals, *J. Phys. Chem. A*, (2), 150923134432004, doi:10.1021/acs.jpca.5b07295, 2015.
- Bianchi, F., Tröstl, J., Junninen, H., Frege, C., Henne, S., Hoyle, C. R., Molteni, U., Herrmann, E., Adamov, A., Bukowiecki, N., Chen, X., Duplissy, J., Gysel, M., Hutterli, M., Kangasluoma, J., Kontkanen, J., Kurten, A., Manninen, H. E., Munch, S., 335 Perakyla, O., Petaja, T., Rondo, L., Williamson, C., Weingartner, E., Curtius, J., Worsnop, D. R., Kulmala, M., Dommen, J. and Baltensperger, U.: New particle formation in the free troposphere: A question of chemistry and timing, *Science* (80), 352(6289), 1109–1112, doi:10.1126/science.aad5456, 2016.
- Birdsall, A. W. and Elrod, M. J.: Comprehensive NO-dependent study of the products of the oxidation of atmospherically relevant aromatic compounds, *J. Phys. Chem. A*, 115(21), 5397–5407, doi:10.1021/jp2010327, 2011.
- 340 Bohn, B.: Formation of peroxy radicals from OH–toluene adducts and O₂, *J. Phys. Chem. A*, 105(25), 6092–6101, doi:10.1021/jp0033972, 2001.
- Bruns, E. A., El Haddad, I., Slowik, J. G., Kilic, D., Klein, F., Baltensperger, U. and Prévôt, A. S. H.: Identification of significant precursor gases of secondary organic aerosols from residential wood combustion, *Sci. Rep.*, 6(February), 27881, doi:10.1038/srep27881, 2016.
- 345 Calvert, J. G., Atkinson, R., Becker, K. H., Kamens, R. M., Seinfeld, J. H., Wallington, T. H. and Yarwood, G.: The mechanisms of atmospheric oxidation of the aromatic hydrocarbons, Oxford University Press., 2002.
- Carslaw, K. S., Lee, L. a, Reddington, C. L., Pringle, K. J., Rap, A., Forster, P. M., Mann, G. W., Spracklen, D. V., Woodhouse, M. T., Regayre, L. and Pierce, J. R.: Large contribution of natural aerosols to uncertainty in indirect forcing, *Nature*, 503(7474), 67–71, doi:10.1038/nature12674, 2013.
- 350 Crouse, J. D., Knap, H. C., Ørnsø, K. B., Jørgensen, S., Paulot, F., Kjaergaard, H. G. and Wennberg, P. O.: Atmospheric fate of methacrolein. 1. peroxy radical isomerization following addition of OH and O₂, *J. Phys. Chem. A*, 116(24), 5756–5762, doi:10.1021/jp211560u, 2012.
- Crouse, J. D., Nielsen, L. B., Jørgensen, S., Kjaergaard, H. G. and Wennberg, P. O.: Autoxidation of organic compounds in the atmosphere, *J. Phys. Chem. Lett.*, 4(20), 3513–3520, doi:10.1021/jz4019207, 2013.

- 355 Donahue, N. M., Ortega, I. K., Chuang, W., Riipinen, I., Riccobono, F., Schobesberger, S., Dommen, J., Baltensperger, U., Kulmala, M., Worsnop, D. R. and Vehkamäki, H.: How do organic vapors contribute to new-particle formation?, *Faraday Discuss.*, 165, 91, doi:10.1039/c3fd00046j, 2013.
- Ehn, M., Thornton, J. a., Kleist, E., Sipilä, M., Junninen, H., Pullinen, I., Springer, M., Rubach, F., Tillmann, R., Lee, B., Lopez-Hilfiker, F., Andres, S., Acir, I.-H., Rissanen, M., Jokinen, T., Schobesberger, S., Kangasluoma, J., Kontkanen, J.,
- 360 Nieminen, T., Kurtén, T., Nielsen, L. B., Jørgensen, S., Kjaergaard, H. G., Canagaratna, M., Maso, M. D., Berndt, T., Petäjä, T., Wahner, A., Kerminen, V.-M., Kulmala, M., Worsnop, D. R., Wildt, J. and Mentel, T. F.: A large source of low-volatility secondary organic aerosol, *Nature*, 506(7489), 476–479, doi:10.1038/nature13032, 2014.
- Glowacki, D. R. and Pilling, M. J.: Unimolecular reactions of peroxy radicals in atmospheric chemistry and combustion, *ChemPhysChem*, 11(18), 3836–3843, doi:10.1002/cphc.201000469, 2010.
- 365 Gordon, H., Sengupta, K., Rap, A., Duplissy, J., Frege, C., Williamson, C., Heinritzi, M., Simon, M., Yan, C., Almeida, J., Tröstl, J., Nieminen, T., Ortega, I. K., Wagner, R., Dunne, E. M., Adamov, A., Amorim, A., Bernhammer, A.-K., Bianchi, F., Breitenlechner, M., Brilke, S., Chen, X., Craven, J. S., Dias, A., Ehrhart, S., Fischer, L., Flagan, R. C., Franchin, A., Fuchs, C., Guida, R., Hakala, J., Hoyle, C. R., Jokinen, T., Junninen, H., Kangasluoma, J., Kim, J., Kirkby, J., Krapf, M., Kürten, A., Laaksonen, A., Lehtipalo, K., Makhmutov, V., Mathot, S., Molteni, U., Monks, S. A., Onnela, A., Peräkylä, O., Piel, F.,
- 370 Petäjä, T., Praplan, A. P., Pringle, K. J., Richards, N. A. D., Rissanen, M. P., Rondo, L., Sarnela, N., Schobesberger, S., Scott, C. E., Seinfeld, J. H., Sharma, S., Sipilä, M., Steiner, G., Stozhkov, Y., Stratmann, F., Tomé, A., Virtanen, A., Vogel, A. L., Wagner, A. C., Wagner, P. E., Weingartner, E., Wimmer, D., Winkler, P. M., Ye, P., Zhang, X., Hansel, A., Dommen, J., Donahue, N. M., Worsnop, D. R., Baltensperger, U., Kulmala, M., Curtius, J. and Carslaw, K. S.: Reduced anthropogenic aerosol radiative forcing caused by biogenic new particle formation, *Proc. Natl. Acad. Sci.*, 201602360, doi:10.1073/pnas.1602360113, 2016.
- Hyttinen, N., Kupiainen-Määttä, O., Rissanen, M. P., Muuronen, M., Ehn, M. and Kurtén, T.: Modeling the charging of highly oxidized cyclohexene ozonolysis products using nitrate-based chemical ionization, *J. Phys. Chem. A*, 119(24), 6339–6345, doi:10.1021/acs.jpca.5b01818, 2015.
- Jain, C., Morajkar, P., Schoemaeker, C. and Fittschen, C.: Formation of HO₂ radicals from the 248 nm two-photon excitation of different aromatic hydrocarbons in the presence of O₂, *J. Phys. Chem. A*, 116(24), 6231–6239, doi:10.1021/jp211520g, 2012.
- 380 Jenkin, M. E., Saunders, S. M., Wagner, V. and Pilling, M. J.: Protocol for the development of the Master Chemical Mechanism, MCM v3 (Part B): tropospheric degradation of aromatic volatile organic compounds, *Atmos. Chem. Phys.*, 3(1), 181–193, doi:10.5194/acp-3-181-2003, 2003.
- 385 Jokinen, T., Sipilä, M., Junninen, H., Ehn, M., Lönn, G., Hakala, J., Petäjä, T., Mauldin, R. L., Kulmala, M. and Worsnop, D. R.: Atmospheric sulphuric acid and neutral cluster measurements using CI-APi-TOF, *Atmos. Chem. Phys.*, 12(9), 4117–4125, doi:10.5194/acp-12-4117-2012, 2012.
- Jokinen, T., Sipilä, M., Richters, S., Kerminen, V.-M., Paasonen, P., Stratmann, F., Worsnop, D., Kulmala, M., Ehn, M., Herrmann, H. and Berndt, T.: Rapid autoxidation forms highly oxidized RO₂ radicals in the atmosphere, *Angew. Chemie Int. Ed.*, 53(52), 14596–14600, doi:10.1002/anie.201408566, 2014.
- 390 Jokinen, T., Berndt, T., Makkonen, R., Kerminen, V., Junninen, H., Paasonen, P., Stratmann, F., Herrmann, H., Guenther, A. B., Worsnop, D. R., Kulmala, M., Ehn, M. and Sipilä, M.: Production of extremely low volatile organic compounds from

- biogenic emissions: Measured yields and atmospheric implications, *Proc. Natl. Acad. Sci.*, 112(23), 7123–7128, doi:10.1073/pnas.1423977112, 2015.
- 395 Jordan, A., Haidacher, S., Hanel, G., Hartungen, E., Märk, L., Seehauser, H., Schotchkowsky, R., Sulzer, P. and Märk, T. D.: A high resolution and high sensitivity proton-transfer-reaction time-of-flight mass spectrometer (PTR-TOF-MS), *Int. J. Mass Spectrom.*, 286(2–3), 122–128, doi:10.1016/j.ijms.2009.07.005, 2009.
- Kirkby, J., Duplissy, J., Sengupta, K., Frege, C., Gordon, H., Williamson, C., Heinritzi, M., Simon, M., Yan, C., Almeida, J., Tröstl, J., Nieminen, T., Ortega, I. K., Wagner, R., Adamov, A., Amorim, A., Bernhammer, A.-K., Bianchi, F., Breitenlechner, M., Brilke, S., Chen, X., Craven, J., Dias, A., Ehrhart, S., Flagan, R. C., Franchin, A., Fuchs, C., Guida, R., Hakala, J., Hoyle, C. R., Jokinen, T., Junninen, H., Kangasluoma, J., Kim, J., Krapf, M., Kürten, A., Laaksonen, A., Lehtipalo, K., Makhmutov, V., Mathot, S., Molteni, U., Onnela, A., Peräkylä, O., Piel, F., Petäjä, T., Praplan, A. P., Pringle, K., Rap, A., Richards, N. A. D., Riipinen, I., Rissanen, M. P., Rondo, L., Sarnela, N., Schobesberger, S., Scott, C. E., Seinfeld, J. H., Sipilä, M., Steiner, G., Stozhkov, Y., Stratmann, F., Tomé, A., Virtanen, A., Vogel, A. L., Wagner, A. C., Wagner, P. E., Weingartner, E., Wimmer, D., Winkler, P. M., Ye, P., Zhang, X., Hansel, A., Dommen, J., Donahue, N. M., Worsnop, D. R., Baltensperger, U., Kulmala, M., Carslaw, K. S. and Curtius, J.: Ion-induced nucleation of pure biogenic particles, *Nature*, 533(7604), 521–526, doi:10.1038/nature17953, 2016.
- Kogelschatz, U.: Silent discharges for the generation of ultraviolet and vacuum ultraviolet excimer radiation, *Pure Appl. Chem.*, 62(9), 1667–1674, doi:10.1351/pac199062091667, 1990.
- 410 Kogelschatz, U.: Ultraviolet excimer radiation from nonequilibrium gas discharges and its application in photophysics, photochemistry and photobiology, *J. Opt. Technol.*, 79(8), 484, doi:10.1364/JOT.79.000484, 2012.
- Kulmala, M., Kontkanen, J., Junninen, H., Lehtipalo, K., Manninen, H. E., Nieminen, T., Petaja, T., Sipila, M., Schobesberger, S., Rantala, P., Franchin, A., Jokinen, T., Jarvinen, E., Aijala, M., Kangasluoma, J., Hakala, J., Aalto, P. P., Paasonen, P., Mikkila, J., Vanhanen, J., Aalto, J., Hakola, H., Makkonen, U., Ruuskanen, T., Mauldin, R. L., Duplissy, J., Vehkamäki, H., Back, J., Kortelainen, A., Riipinen, I., Kurten, T., Johnston, M. V., Smith, J. N., Ehn, M., Mentel, T. F., Lehtinen, K. E. J., Laaksonen, A., Kerminen, V.-M. and Worsnop, D. R.: Direct observations of atmospheric aerosol nucleation, *Science* (80-.), 339(6122), 943–946, doi:10.1126/science.1227385, 2013.
- Kürten, a., Rondo, L., Ehrhart, S. and Curtius, J.: Performance of a corona ion source for measurement of sulfuric acid by chemical ionization mass spectrometry, *Atmos. Meas. Tech.*, 4, 437–443, doi:10.5194/amt-4-437-2011, 2011.
- 420 Kurtén, T., Rissanen, M. P., Mackeprang, K., Thornton, J. A., Hyttinen, N., Jørgensen, S., Ehn, M. and Kjaergaard, H. G.: Computational study of hydrogen shifts and ring-opening mechanisms in α -pinene ozonolysis products, *J. Phys. Chem. A*, 119(46), 11366–11375, doi:10.1021/acs.jpca.5b08948, 2015.
- Lee, B. H., Mohr, C., Lopez-Hilfiker, F. D., Lutz, A., Hallquist, M., Lee, L., Romer, P., Cohen, R. C., Iyer, S., Kurtén, T., Hu, W., Day, D. A., Campuzano-Jost, P., Jimenez, J. L., Xu, L., Ng, N. L., Guo, H., Weber, R. J., Wild, R. J., Brown, S. S., Koss, A., de Gouw, J., Olson, K., Goldstein, A. H., Seco, R., Kim, S., McAvey, K., Shepson, P. B., Starn, T., Baumann, K., Edgerton, E. S., Liu, J., Shilling, J. E., Miller, D. O., Brune, W., Schobesberger, S., D'Ambro, E. L. and Thornton, J. A.: Highly functionalized organic nitrates in the southeast United States: Contribution to secondary organic aerosol and reactive nitrogen budgets, *Proc. Natl. Acad. Sci.*, 113(6), 1516–1521, doi:10.1073/pnas.1508108113, 2016.

- Li, L., Tang, P., Nakao, S., Kacarab, M. and Cocker, D. R.: Novel approach for evaluating secondary organic aerosol from aromatic hydrocarbons: unified method for predicting aerosol composition and formation, *Environ. Sci. Technol.*, 50(12), 6249–6256, doi:10.1021/acs.est.5b05778, 2016.
- Lightfoot, P., Cox, R., Crowley, J., Destriau, M., Hayman, G., Jenkin, M., Moortgat, G. and Zabel, F.: Organic peroxy radicals: kinetics, spectroscopy and tropospheric chemistry, *Atmos. Environ. Part A. Gen. Top.*, 26(10), 1805–1961, doi:10.1016/0960-1686(92)90423-I, 1992.
- 435 Mentel, T. F., Springer, M., Ehn, M., Kleist, E., Pullinen, I., Kurtén, T., Rissanen, M., Wahner, A. and Wildt, J.: Formation of highly oxidized multifunctional compounds: autoxidation of peroxy radicals formed in the ozonolysis of alkenes – deduced from structure–product relationships, *Atmos. Chem. Phys.*, 15(12), 6745–6765, doi:10.5194/acp-15-6745-2015, 2015.
- Metzger, A., Verheggen, B., Dommen, J., Duplissy, J., Prevot, A. S. H., Weingartner, E., Riipinen, I., Kulmala, M., Spracklen, D. V., Carslaw, K. S. and Baltensperger, U.: Evidence for the role of organics in aerosol particle formation under atmospheric conditions, *Proc. Natl. Acad. Sci.*, 107(15), 6646–6651, doi:10.1073/pnas.0911330107, 2010.
- 440 Molina, M. J., Zhang, R., Broekhuizen, K., Lei, W., Navarro, R. and Molina, L. T.: Experimental study of intermediates from OH-initiated reactions of toluene, *J. Am. Chem. Soc.*, 121(43), 10225–10226, doi:10.1021/ja992461u, 1999.
- Nakao, S., Clark, C., Tang, P., Sato, K. and Cocker, D.: Secondary organic aerosol formation from phenolic compounds in the absence of NO_x, *Atmos. Chem. Phys.*, 11(20), 10649–10660, doi:10.5194/acp-11-10649-2011, 2011.
- 445 Orlando, J. J. and Tyndall, G. S.: Laboratory studies of organic peroxy radical chemistry: an overview with emphasis on recent issues of atmospheric significance, *Chem. Soc. Rev.*, 41(19), 6294, doi:10.1039/c2cs35166h, 2012.
- Pan, S. and Wang, L.: Atmospheric oxidation mechanism of m-xylene initiated by OH radical, *J. Phys. Chem. A*, 118(45), 10778–10787, doi:10.1021/jp506815v, 2014.
- Peng, Z., Day, D. A., Ortega, A. M., Palm, B. B., Hu, W., Stark, H., Li, R., Tsigaridis, K., Brune, W. H. and Jimenez, J. L.: Non-OH chemistry in oxidation flow reactors for the study of atmospheric chemistry systematically examined by modelling, *Atmos. Chem. Phys.*, 16(7), 4283–4305, doi:10.5194/acp-16-4283-2016, 2016.
- 455 Praplan, a. P., Schobesberger, S., Bianchi, F., Rissanen, M. P., Ehn, M., Jokinen, T., Junninen, H., Adamov, A., Amorim, A., Dommen, J., Duplissy, J., Hakala, J., Hansel, A., Heinritzi, M., Kangasluoma, J., Kirkby, J., Krapf, M., Kürten, A., Lehtipalo, K., Riccobono, F., Rondo, L., Sarnela, N., Simon, M., Tomé, A., Tröstl, J., Winkler, P. M., Williamson, C., Ye, P., Curtius, J., Baltensperger, U., Donahue, N. M., Kulmala, M. and Worsnop, D. R.: Elemental composition and clustering behaviour of α -pinene oxidation products for different oxidation conditions, *Atmos. Chem. Phys.*, 15(8), 4145–4159, doi:10.5194/acp-15-4145-2015, 2015.
- Pratte, P. and Rossi, M. J.: The heterogeneous kinetics of HOBr and HOCl on acidified sea salt and model aerosol at 40–90% relative humidity and ambient temperature, *Phys. Chem. Chem. Phys.*, 8(34), 3988–4001, doi:10.1039/B604321F, 2006.
- 460 Richters, S., Herrmann, H. and Berndt, T.: Highly oxidized RO₂ radicals and consecutive products from the ozonolysis of three sesquiterpenes, *Environ. Sci. Technol.*, 50(5), 2354–2362, doi:10.1021/acs.est.5b05321, 2016.
- Rissanen, M. P., Kurtén, T., Sipilä, M., Thornton, J. A., Kangasluoma, J., Sarnela, N., Junninen, H., Jørgensen, S., Schallhart, S., Kajos, M. K., Taipale, R., Springer, M., Mentel, T. F., Ruuskanen, T., Petäjä, T., Worsnop, D. R., Kjaergaard, H. G. and

- Ehn, M.: The formation of highly oxidized multifunctional products in the ozonolysis of cyclohexene, *J. Am. Chem. Soc.*, 465 136(44), 15596–15606, doi:10.1021/ja507146s, 2014.
- Rissanen, M. P., Kurtén, T., Sipilä, M., Thornton, J. a., Kausiala, O., Garmash, O., Kjaergaard, H. G., Petäjä, T., Worsnop, D. R., Ehn, M. and Kulmala, M.: Effects of chemical complexity on the autoxidation mechanisms of endocyclic alkene ozonolysis products: from methylcyclohexenes toward understanding α -pinene, *J. Phys. Chem. A*, 119(19), 4633–4650, doi:10.1021/jp510966g, 2015.
- 470 Salvermoser, M., Murnick, D. E. and Kogelschatz, U.: Influence of water vapor on photochemical ozone generation with efficient 172 nm xenon excimer lamps, *ozone Sci. Eng.*, 30(3), 228–237, doi:10.1080/01919510802070611, 2008.
- Schwantes, R. H., Schilling, K. A., McVay, R. C., Lignell, H., Coggon, M. M., Zhang, X., Wennberg, P. O. and Seinfeld, J. H.: Formation of highly oxygenated low-volatility products from cresol oxidation, *Atmos. Chem. Phys. Discuss.*, 7(October), 1–34, doi:10.5194/acp-2016-887, 2016.
- 475 Stanier, C. O., Khlystov, A. Y. and Pandis, S. N.: Nucleation events during the Pittsburgh air quality study: description and relation to key meteorological, gas phase, and aerosol parameters special issue of aerosol science and technology on findings from the fine particulate matter supersites program, *Aerosol Sci. Technol.*, 38(sup1), 253–264, doi:10.1080/02786820390229570, 2004.
- Suh, I., Zhang, R., Molina, L. T. and Molina, M. J.: Oxidation mechanism of aromatic peroxy and bicyclic radicals from OH-toluene reactions, *J. Am. Chem. Soc.*, 125(41), 12655–12665, doi:10.1021/ja0350280, 2003.
- Tröstl, J., Chuang, W. K., Gordon, H., Heinritzi, M., Yan, C., Molteni, U., Ahlm, L., Frege, C., Bianchi, F., Wagner, R., Simon, M., Lehtipalo, K., Williamson, C., Craven, J. S., Duplissy, J., Adamov, A., Almeida, J., Bernhammer, A.-K., Breitenlechner, M., Brilke, S., Dias, A., Ehrhart, S., Flagan, R. C., Franchin, A., Fuchs, C., Guida, R., Gysel, M., Hansel, A., Hoyle, C. R., Jokinen, T., Junninen, H., Kangasluoma, J., Keskinen, H., Kim, J., Krapf, M., Kürten, A., Laaksonen, A., 485 Lawler, M., Leiminger, M., Mathot, S., Möhler, O., Nieminen, T., Onnela, A., Petäjä, T., Piel, F. M., Miettinen, P., Rissanen, M. P., Rondo, L., Sarnela, N., Schobesberger, S., Sengupta, K., Sipilä, M., Smith, J. N., Steiner, G., Tomè, A., Virtanen, A., Wagner, A. C., Weingartner, E., Wimmer, D., Winkler, P. M., Ye, P., Carslaw, K. S., Curtius, J., Dommen, J., Kirkby, J., Kulmala, M., Riipinen, I., Worsnop, D. R., Donahue, N. M. and Baltensperger, U.: The role of low-volatility organic compounds in initial particle growth in the atmosphere, *Nature*, 533(7604), 527–531, doi:10.1038/nature18271, 2016.
- 490 Vereecken, L. and Peeters, J.: Decomposition of substituted alkoxy radicals – part I: a generalized structure-activity relationship for reaction barrier heights., *Phys. Chem. Chem. Phys.*, 11(40), 9062–9074, doi:10.1039/b909712k, 2009.
- Wallington, T. J., Dagaut, P. and Kurylo, M. J.: UV absorption cross sections and reaction kinetics and mechanisms for peroxy radicals in the gas phase, *Chem. Rev.*, 92(4), 667–710, doi:10.1021/cr00012a008, 1992.
- Wang, Z. B., Hu, M., Pei, X. Y., Zhang, R. Y., Paasonen, P., Zheng, J., Yue, D. L., Wu, Z. J., Boy, M. and Wiedensohler, A.: 495 Connection of organics to atmospheric new particle formation and growth at an urban site of Beijing, *Atmos. Environ.*, 103, 7–17, doi:10.1016/j.atmosenv.2014.11.069, 2015.
- Xiao, S., Wang, M. Y., Yao, L., Kulmala, M., Zhou, B., Yang, X., Chen, J. M., Wang, D. F., Fu, Q. Y., Worsnop, D. R. and Wang, L.: Strong atmospheric new particle formation in winter in urban Shanghai, China, *Atmos. Chem. Phys.*, 15(4), 1769–1781, doi:10.5194/acp-15-1769-2015, 2015.

500 Yu, H., Zhou, L., Dai, L., Shen, W., Dai, W., Zheng, J., Ma, Y. and Chen, M.: Nucleation and growth of sub-3 nm particles in the polluted urban atmosphere of a megacity in China, *Atmos. Chem. Phys.*, 16(4), 2641–2657, doi:10.5194/acp-16-2641-2016, 2016.

Tables

505 **Table 1** Initial concentrations of precursors and reaction rate coefficients. The mixing ratio was determined at the exit of the flow tube when the excimer lamp (OH generation) was switched off.

Compound	Concentration (molecules·cm ⁻³)	k _{-OH} (10 ⁻¹² ·cm ³ ·molecules ⁻¹ ·s ⁻¹)	k _{-O3} (10 ⁻¹⁷ ·cm ³ ·molecules ⁻¹ ·s ⁻¹)
Benzene (C ₆ H ₆)	9.85·10 ¹³	1.22	<1·10 ⁻³
Toluene (C ₇ H ₈)	1.97·10 ¹³	5.63	<1·10 ⁻³
Ethylbenzene (C ₈ H ₁₀)	1.13·10 ¹³	7.0	<1·10 ⁻³
(o/m/p)-xylene (C ₈ H ₁₀)	2.95·10 ¹²	13.6/23.1/14.3	<1·10 ⁻³
Mesitylene (C ₉ H ₁₂)	2.46·10 ¹²	56.7	<1·10 ⁻³
Naphthalene (C ₁₀ H ₈)	2.95·10 ¹³	23.0	<0.02
Biphenyl (C ₁₂ H ₁₀)	4.43·10 ¹³	7.1	<0.02

510 Initial concentrations of precursors, reaction rate coefficients, ArHC reacted fraction (%), total HOMs concentration and HOMs yield (%) relative to the reacted ArHC. The mixing ratio of precursors was determined at the exit of the flow tube when the excimer lamp (OH generation) was switched off.

<u>Compound</u>	<u>Concentration</u> (molecules cm ⁻³)	<u>k_{OH}</u> (10 ⁻¹² cm ³ molecules ⁻¹ s ⁻¹)	<u>Reacted fraction</u> (%)	<u>[HOM]</u> (molecules cm ⁻³)	<u>HOMs yield</u> (%)
<u>Benzene (C₆H₆)</u>	<u>9.85 10¹³</u>	<u>1.22</u>	<u>0.5</u>	<u>1.2 10⁹</u>	<u>0.2</u>
<u>Toluene (C₇H₈)</u>	<u>1.97 10¹³</u>	<u>5.63</u>	<u>2.3</u>	<u>4.4 10⁸</u>	<u>0.1</u>
<u>Ethylbenzene (C₈H₁₀)</u>	<u>1.13 10¹³</u>	<u>7.0</u>	<u>2.8</u>	<u>9.4 10⁸</u>	<u>0.3</u>
<u>(o/m/p)-xylene (C₈H₁₀)</u>	<u>2.95 10¹²</u>	<u>13.6/23.1/14.3</u>	<u>//</u>	<u>2.8 10⁹</u>	<u>//</u>
<u>Mesitylene (C₉H₁₂)</u>	<u>2.46 10¹²</u>	<u>56.7</u>	<u>22.7</u>	<u>3.1 10⁹</u>	<u>0.6</u>
<u>Naphthalene (C₁₀H₈)</u>	<u>2.95 10¹³</u>	<u>23.0</u>	<u>9.2</u>	<u>1.4 10¹⁰</u>	<u>0.5</u>
<u>Biphenyl (C₁₂H₁₀)</u>	<u>4.43 10¹³</u>	<u>7.1</u>	<u>2.8</u>	<u>1.8 10¹⁰</u>	<u>1.4</u>

Reference for the *k*-rates: (Atkinson and Arey, 2003)

Table 2

Summary of HOM characteristics. For each of the 7 compounds the percentage fractional distribution of the signal is presented. For monocyclic compounds the distribution comprises monomers and dimers, for naphthalene and biphenyl monomers, dimers, trimers and tetramers are reported. These values are not quantitative as the instrument cannot be calibrated for such compounds. For each band the weighted arithmetic means of the O:C ratio are reported in parentheses. The fraction of the identified peaks as adduct with NO_3^- is given in the last column.

Compound	Bands distribution				Adduct ($\text{HOM}\cdot\text{NO}_3^-$)
	Monomer (O:C)	Dimer (O:C)	Trimer (O:C)	Tetramer (O:C)	
Benzene (C_6H_6)	0.80 (1.08)	0.20 (0.91)			0.91
Toluene (C_7H_8)	0.71 (1.09)	0.29 (0.75)			0.94
Ethylbenzene (C_8H_{10})	0.69 (0.86)	0.31 (0.62)			0.83
(o/m/p)-xylene (C_8H_{10})	0.65 (0.78)	0.35 (0.57)			0.92
Mesitylene (C_9H_{12})	0.61 (0.81)	0.39 (0.49)			0.92
	Monomer (O:C)	Dimer (O:C)	Trimer (O:C)	Tetramer (O:C)	
Naphthalene (C_{10}H_8)	0.34 (0.55)	0.64 (0.29)	0.02 (0.34)	0.01 (0.28)	0.84
Biphenyl ($\text{C}_{12}\text{H}_{10}$)	0.52 (0.44)	0.43 (0.35)	0.04 (0.29)	0.01 (0.32)	0.77

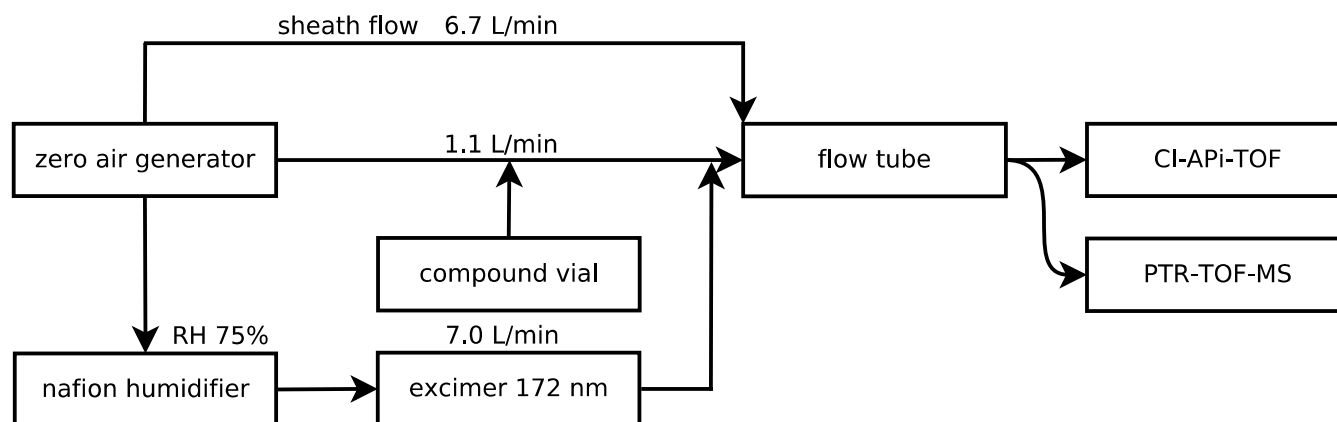


Figure 1. Experimental set-up. Zero air from a pure air generator is split into 3 flows. A sheath flow of 6.7 L min^{-1} . An air stream of 1.1 L min^{-1} collects vapours from a reagent compound vial and is then mixed with a humidified air stream of 7 L min^{-1} (RH 75%) which carries OH free radicals generated through irradiation at 172 nm.

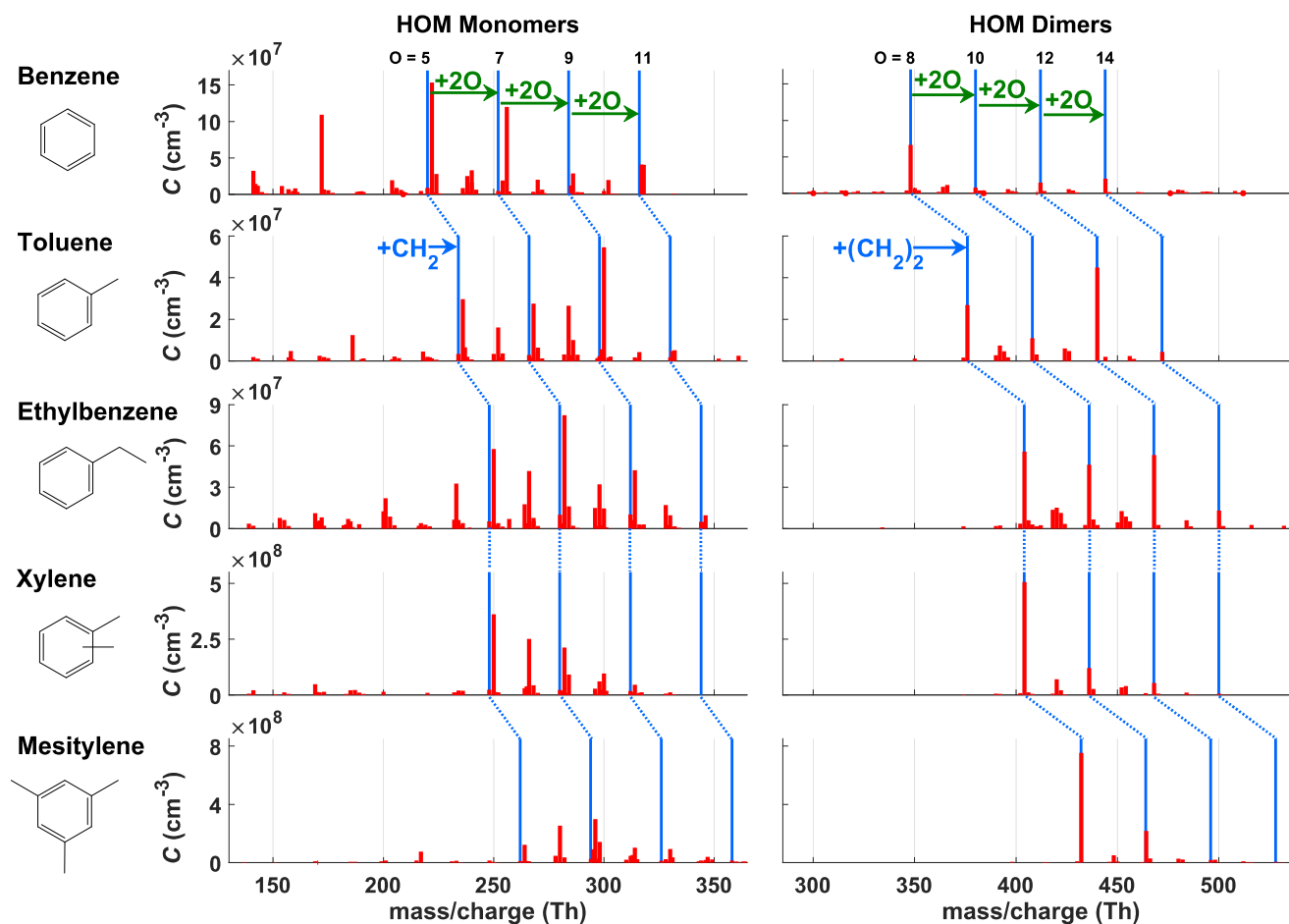


Figure 2. HOMs from 5 monocyclic ArHC (benzene, toluene, ethylbenzene, xylenes, mesitylene). HOM monomers ([left panel](#)) have the same number of carbon atoms as the precursor while HOM dimers ([right panel](#)) have twice as many. Green arrows in the benzene panel show a sequence of peaks separated by a mass corresponding to 2 oxygen atoms. This may be connected to the autoxidation mechanism which proceeds through addition of O_2 molecules. The same sequence is seen in the other ArHCs as indicated by the blue lines. The initial peak and the corresponding sequence of the 5 single-ring ArHC are shifted by a CH_2 unit due to the different substituents (blue arrow in the toluene panel). **HOM peaks (in red) are not always aligned to the blue lines due to the unequal prevalence of HOMs with the same number of oxygen atoms can have a different number of hydrogen atoms ($n, n+2, n+4$).** Note the different peak intensity patterns observed for the different chemical compounds, even for xylene and ethylbenzene, i.e., molecules with the same chemical formula.

540

Polycyclic ArHC

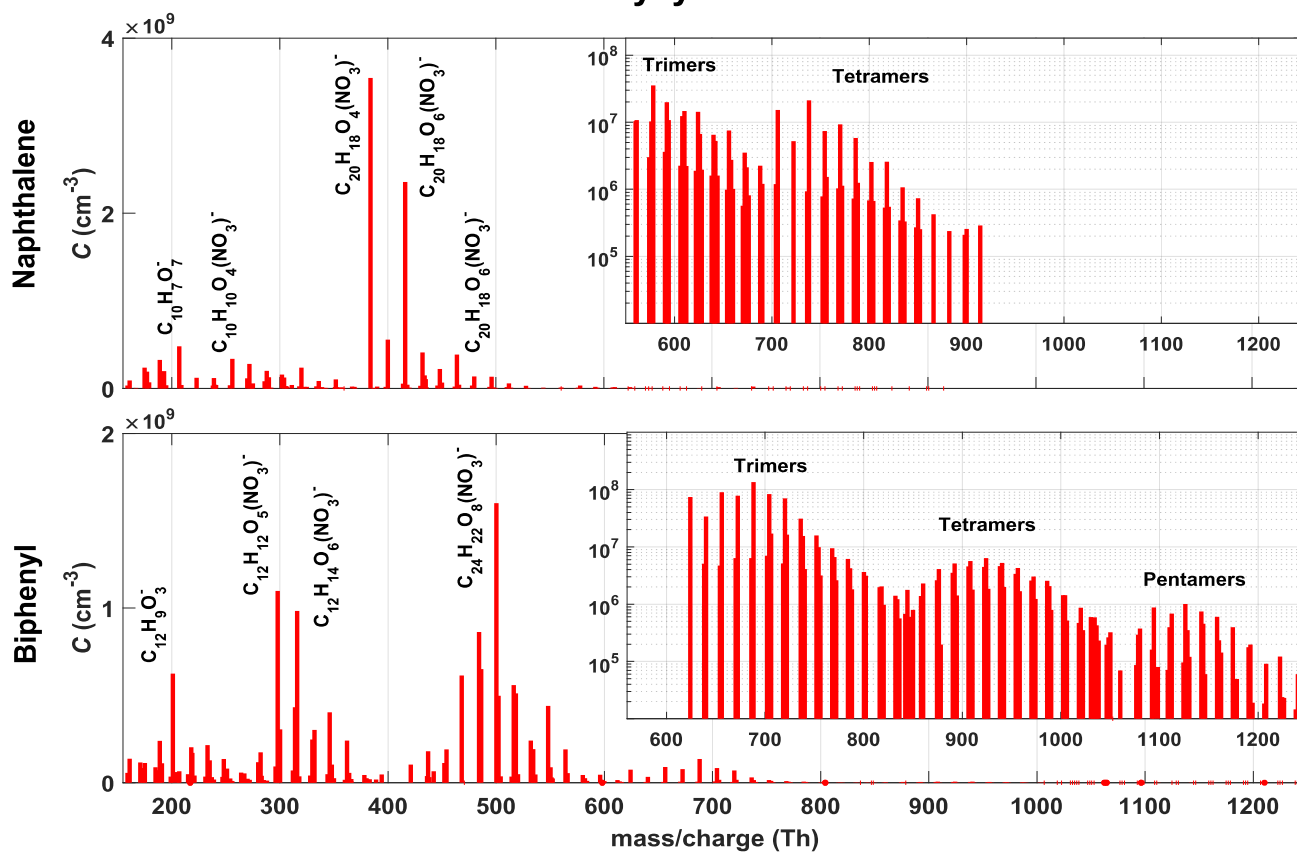


Figure 3. Mass spectra of HOMs from the bicyclic ArHC naphthalene and biphenyl. The chemical composition of some representative peaks is displayed. Due to the high concentrations the nitrate CI-API-TOF was also able to ~~also~~ detect the HOMs clusters up to the pentamer and also retrieve their chemical formula (see inserts).

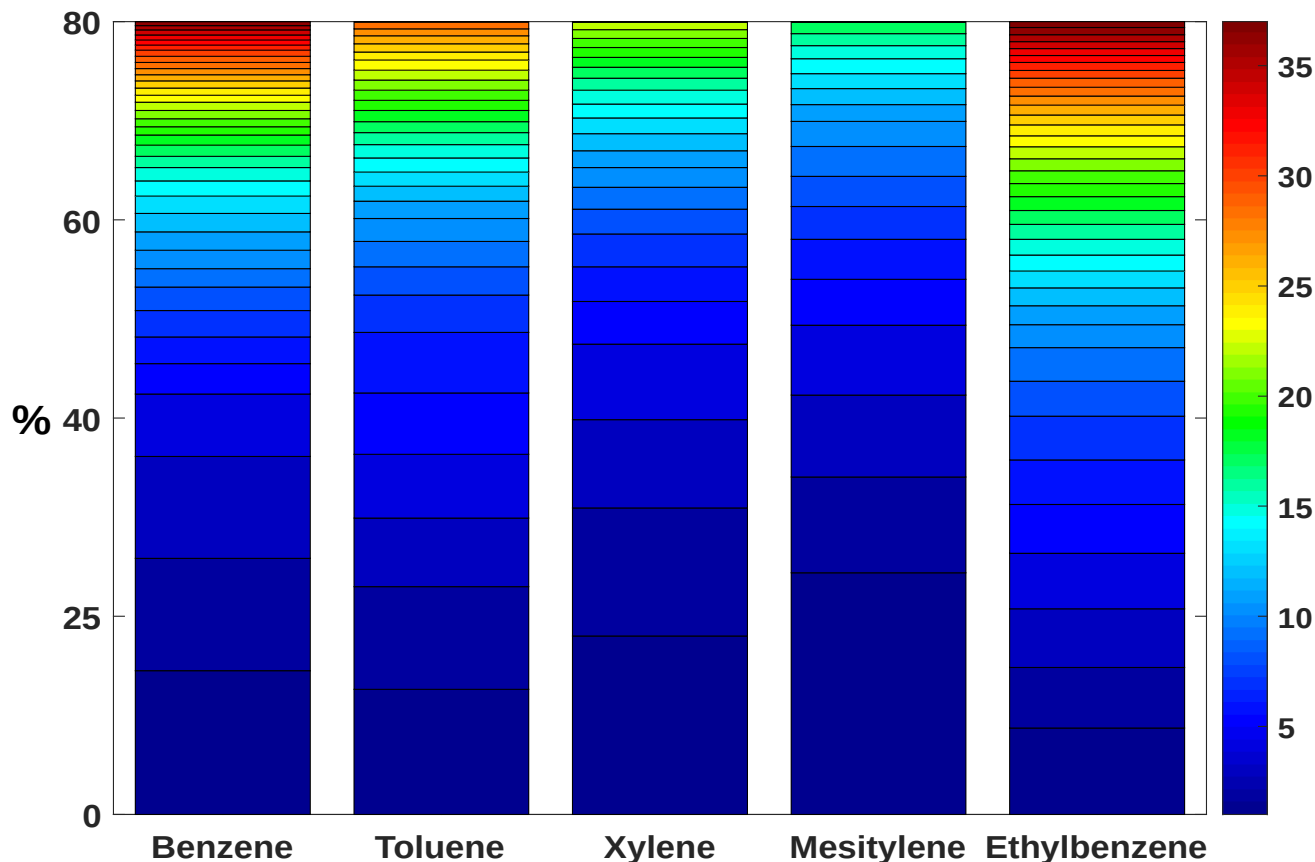


Figure 4. Graphical representation of the cumulative peak lists for the 5 monocyclic ArHC. The bar plot shows the cumulative contribution of the most abundant HOMs species to 80% of the total detected signal for each single-ring ArHC.

550 Each colour of the stacked bar plots denotes a certain number of cumulative compounds. In the series benzene, toluene, xylene and mesitylene a gradually smaller number of different HOM species is needed to explain 80% of the total signal. ~~Ethylbenzene does not follow this empirical observation and shows the highest number of HOMs in these 80%~~ However, this trend with the increase of the number of substituents is not met by ethylbenzene. This may be linked to the fact that dimers with an unexpectedly low number of hydrogen were observed. Ethylbenzene shows a lower fraction of HOM·NO₃⁻ adducts

555 as well.

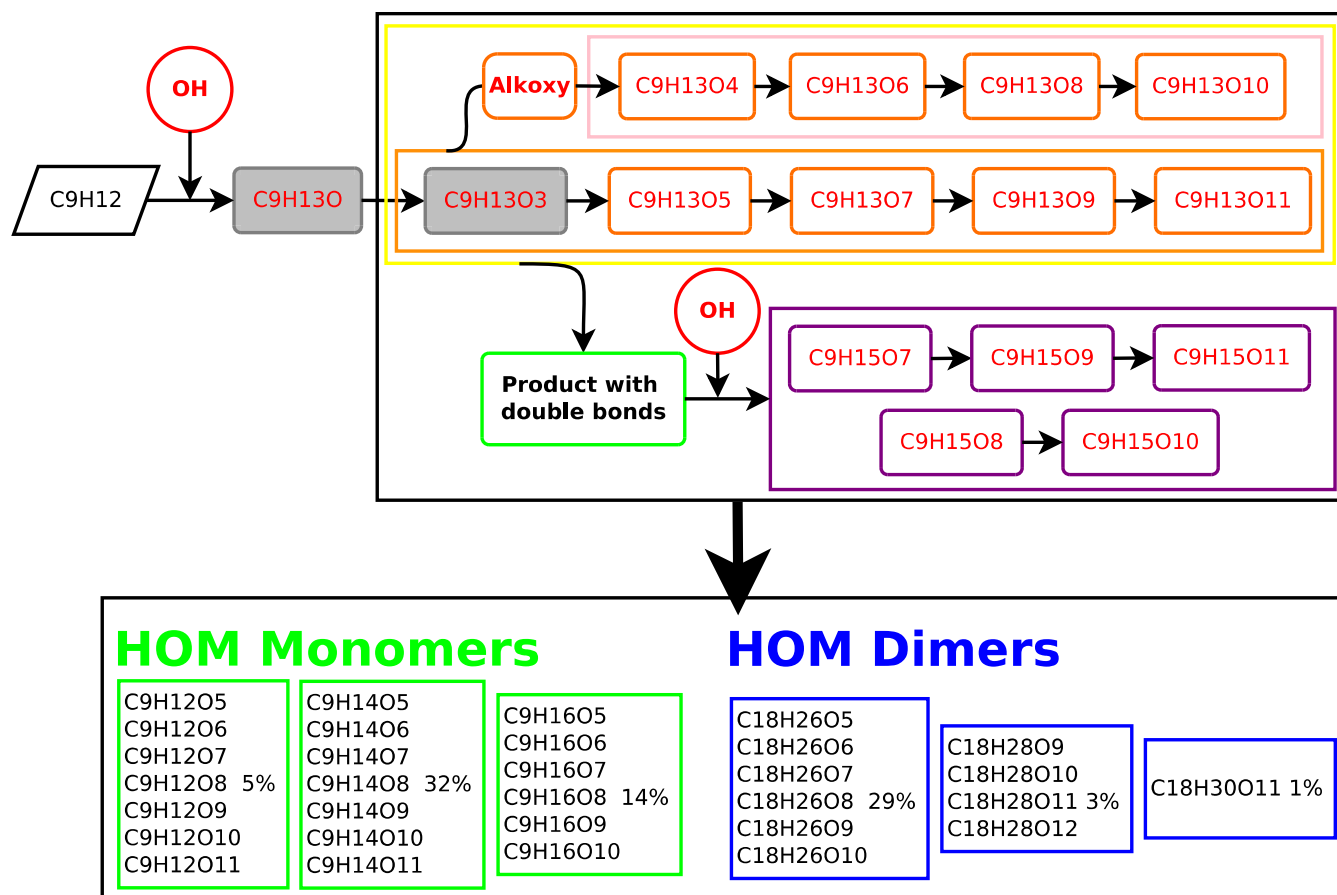


Figure 5 Proposed generalized reaction scheme of HOM formation for mesitylene (1,3,5-trimethylbenzene) after OH addition. In black closed-shell species (even number of H), in red radicals (odd number of H). Grey colour denotes radicals that were not detected by the CIMS. Radicals in the orange box are from the propagation of the initial OH attack with an odd number of oxygen atoms, radicals in the pink box are formed via an alkoxy intermediate step with an even number of oxygen atoms, while radicals in the purple box are products of a second OH addition. Radicals in the orange box are from the propagation of the initial OH attack with an odd number of oxygen, radicals in the yellow box are first generation products with an even number of oxygen, while radicals in the purple boxes are products of a secondary OH addition. Reacting oxygen molecules along the radical propagation chain are not indicated. Closed-shell species are divided into monomers (green boxes) and dimers (blue boxes). The percentages in the boxes indicate the relative intensity of a peak to the total detected ArHC HOMs signal. The sum does not add up to 100% because some peaks mainly coming from fragmentation are not included in the scheme.

570

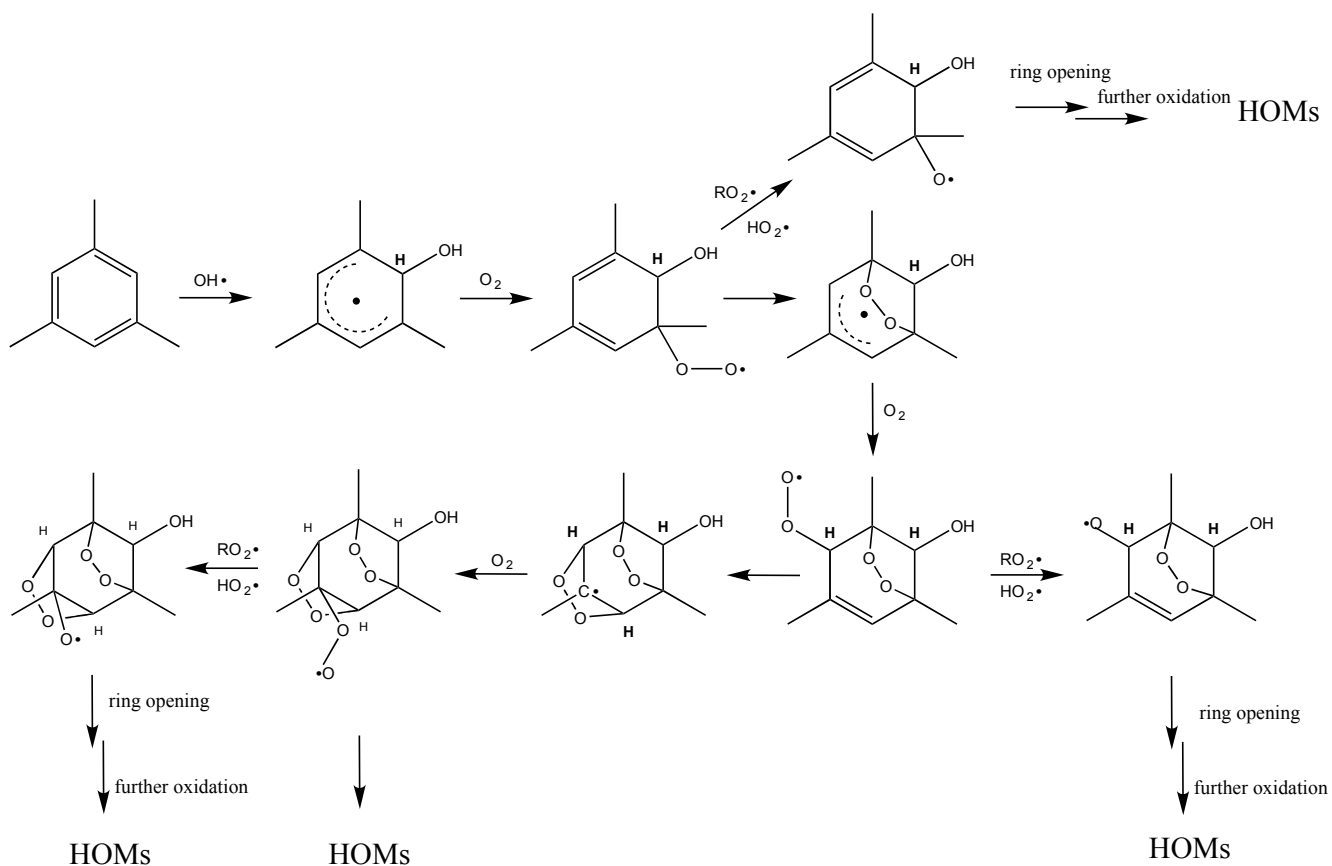


Figure 6. Proposed radical reaction mechanism for the autoxidation of mesitylene. The mechanism is derived from the MCM (version 3.3.1) and takes into account 1st generation radicals. The mechanism is intended to represent just one possibility; other paths are reasonable as well but not shown here.

Appendix A

580 Peak lists of the most abundant HOMs of each ArHC tested are presented in the next 7 tables. The peaks are sorted with decreasing relative intensity. Chemical formula, exact mass and fraction of the explained signal are included. The exact mass includes the mass of NO₃ if present.

Table A-1

CI-API-TOF peak list for benzene (C₆H₆) oxidation products.

Chemical formula	Mass	Fraction of explained signal
C ₆ H ₈ O ₅ (NO ₃) ⁻	222.0255	14.1
C ₃ H ₆ O ₈ (NO ₃) ⁻	255.9946	11.0
C ₆ H ₆ O ₂ (NO ₃) ⁻	172.0251	10.0
C ₁₂ H ₁₄ O ₈ (NO ₃) ⁻	348.0572	6.1
C ₃ H ₆ O ₇ (NO ₃) ⁻	239.9997	3.0
C ₆ H ₈ O ₉ (NO ₃) ⁻	286.0052	2.6
C ₃ H ₆ O ₆ (NO ₃) ⁻	224.0048	2.6
C ₆ H ₈ O ₆ (NO ₃) ⁻	238.0205	2.3
C ₆ H ₈ O ₈ (NO ₃) ⁻	270.0103	1.8
C ₁₂ H ₁₄ O ₁₄ (NO ₃) ⁻	444.0267	1.8
C ₆ H ₈ O ₁₀ (NO ₃) ⁻	302.0001	1.8
C ₆ H ₆ O ₄ (NO ₃) ⁻	204.0150	1.8
C ₆ H ₈ O ₇ (NO ₃) ⁻	254.0154	1.7
C ₆ H ₁₀ O ₆ (NO ₃) ⁻	240.0361	1.5
C ₁₂ H ₁₄ O ₁₂ (NO ₃) ⁻	412.0369	1.3
C ₆ H ₇ O ₉ (NO ₃) ⁻	284.9974	1.1
C ₆ H ₇ O ₄ ⁻	143.0350	1.1
C ₁₂ H ₁₆ O ₉ (NO ₃) ⁻	366.0678	1.0
C ₆ H ₈ O ₄ (NO ₃) ⁻	206.0306	0.8
C ₆ H ₆ O ₅ (NO ₃) ⁻	220.0099	0.8
C ₁₂ H ₁₄ O ₉ (NO ₃) ⁻	364.0522	0.8
C ₆ H ₆ O ₆ (NO ₃) ⁻	236.0048	0.8
C ₃ H ₆ O ₂ (NO ₃) ⁻	160.0251	0.7
C ₁₂ H ₁₄ O ₁₀ (NO ₃) ⁻	380.0471	0.7
C ₆ H ₅ O ₅ ⁻	157.0143	0.7
C ₁₂ H ₁₆ O ₈ (NO ₃) ⁻	350.0729	0.6
C ₆ H ₅ O ₆ ⁻	173.0092	0.6
C ₃ H ₈ O ₇ (NO ₃) ⁻	242.0154	0.6
C ₆ H ₁₀ O ₈ (NO ₃) ⁻	272.0259	0.6
C ₃ H ₆ O ₅ (NO ₃) ⁻	208.0099	0.6
C ₁₂ H ₁₄ O ₁₁ (NO ₃) ⁻	396.0420	0.5
C ₁₂ H ₁₂ O ₁₃ (NO ₃) ⁻	426.0161	0.5
C ₆ H ₇ O ₆ ⁻	175.0248	0.5
C ₁₀ H ₁₀ O ₁₈ (NO ₃) ⁻	479.9751	0.5
C ₆ H ₇ O ₄ (NO ₃) ⁻	205.0228	0.4

$C_6H_6O_7(NO_3)^-$	251.9997	0.4
---------------------	----------	-----

585

Table A-2CI-API-TOF peak list for toluene (C₇H₈) oxidation products.

Chemical formula	Mass	Fraction of explained signal
C ₇ H ₁₀ O ₉ (NO ₃) ⁻	300.0208	12.4
C ₁₄ H ₁₈ O ₁₂ (NO ₃) ⁻	440.0682	10.2
C ₇ H ₁₀ O ₅ (NO ₃) ⁻	236.0412	6.8
C ₇ H ₁₀ O ₇ (NO ₃) ⁻	268.0310	6.3
C ₁₄ H ₁₈ O ₈ (NO ₃) ⁻	376.0885	6.1
C ₇ H ₁₀ O ₈ (NO ₃) ⁻	284.0259	6.0
C ₇ H ₁₀ O ₆ (NO ₃) ⁻	252.0361	3.7
C ₇ H ₈ O ₂ (NO ₃) ⁻	186.0408	2.8
C ₁₄ H ₁₈ O ₁₀ (NO ₃) ⁻	408.0784	2.5
C ₇ H ₁₂ O ₈ (NO ₃) ⁻	286.0416	2.3
C ₁₄ H ₁₈ O ₉ (NO ₃) ⁻	392.0834	1.7
C ₆ H ₇ O ₆ (NO ₃) ⁻	237.0126	1.5
C ₇ H ₁₂ O ₇ (NO ₃) ⁻	270.0467	1.4
C ₁₄ H ₁₈ O ₁₁ (NO ₃) ⁻	424.0733	1.4
C ₇ H ₉ O ₉ (NO ₃) ⁻	299.0130	1.3
C ₇ H ₁₀ O ₁₁ (NO ₃) ⁻	332.0107	1.2
C ₇ H ₉ O ₁₁ (NO ₃) ⁻	331.0029	1.1
C ₆ H ₆ O ₅ ⁻	158.0215	1.1
C ₁₄ H ₂₀ O ₁₁ (NO ₃) ⁻	426.0889	1.1
C ₁₄ H ₂₀ O ₉ (NO ₃) ⁻	394.0991	1.0
C ₇ H ₈ O ₄ (NO ₃) ⁻	218.0306	1.0
C ₆ H ₈ O ₈ (NO ₃) ⁻	270.0103	1.0
C ₁₄ H ₁₈ O ₁₄ (NO ₃) ⁻	472.0580	1.0
C ₇ H ₁₀ O ₁₀ (NO ₃) ⁻	316.0158	1.0
C ₇ H ₁₂ O ₆ (NO ₃) ⁻	254.0518	0.8
C ₇ H ₈ O ₅ (NO ₃) ⁻	234.0255	0.8
C ₇ H ₈ O ₆ (NO ₃) ⁻	250.0205	0.8
C ₁₄ H ₂₀ O ₁₀ (NO ₃) ⁻	410.0940	0.7
C ₇ H ₈ O ₈ (NO ₃) ⁻	282.0103	0.7

CI-API-TOF peak list for ethylbenzene (C₈H₁₀) oxidation products.

Chemical formula	Mass	Fraction of explained signal
C ₈ H ₁₂ O ₇ (NO ₃) ⁻	282.0467	8.7
C ₈ H ₁₂ O ₅ (NO ₃) ⁻	250.0568	6.1
C ₁₆ H ₂₂ O ₈ (NO ₃) ⁻	404.1198	5.9
C ₁₆ H ₂₂ O ₁₂ (NO ₃) ⁻	468.0995	5.6
C ₁₆ H ₂₂ O ₁₀ (NO ₃) ⁻	436.1096	4.9
C ₈ H ₁₂ O ₉ (NO ₃) ⁻	314.0365	4.5
C ₈ H ₁₂ O ₆ (NO ₃) ⁻	266.0518	4.4
C ₈ H ₉ O ₈ ⁻	233.0303	3.5
C ₈ H ₁₂ O ₈ (NO ₃) ⁻	298.0416	3.4
C ₈ H ₉ O ₆ ⁻	201.0405	2.3
C ₈ H ₁₀ O ₆ (NO ₃) ⁻	264.0361	1.9
C ₈ H ₁₀ O ₁₀ (NO ₃) ⁻	328.0158	1.8
C ₈ H ₁₄ O ₇ (NO ₃) ⁻	284.0623	1.7
C ₁₆ H ₂₂ O ₉ (NO ₃) ⁻	420.1147	1.6
C ₈ H ₁₀ O ₈ (NO ₃) ⁻	296.0259	1.6
C ₈ H ₁₄ O ₈ (NO ₃) ⁻	300.0572	1.5
C ₁₆ H ₂₀ O ₉ (NO ₃) ⁻	418.0991	1.4
C ₁₆ H ₂₂ O ₁₄ (NO ₃) ⁻	500.0893	1.4
C ₁₆ H ₂₂ O ₁₁ (NO ₃) ⁻	452.1046	1.3
C ₈ H ₁₀ O ₂ (NO ₃) ⁻	200.0564	1.3
C ₁₆ H ₂₄ O ₉ (NO ₃) ⁻	422.1304	1.2
C ₈ H ₉ O ₄ ⁻	169.0506	1.2
C ₈ H ₁₀ O ₉ (NO ₃) ⁻	312.0208	1.1
C ₈ H ₁₀ O ₇ (NO ₃) ⁻	280.0310	1.1
C ₈ H ₁₂ O ₁₁ (NO ₃) ⁻	346.0263	1.0
C ₈ H ₁₂ O ₁₀ (NO ₃) ⁻	330.0314	1.0
C ₈ H ₁₁ O ₆ ⁻	203.0561	0.9
C ₁₆ H ₂₄ O ₁₁ (NO ₃) ⁻	454.1202	0.9
C ₇ H ₈ O ₅ ⁻	172.0377	0.9
C ₈ H ₉ O ₃ ⁻	153.0557	0.8
C ₈ H ₁₄ O ₆ (NO ₃) ⁻	268.0674	0.8
C ₈ H ₈ O ₅ ⁻	184.0377	0.7
C ₁₆ H ₂₄ O ₁₀ (NO ₃) ⁻	438.1253	0.7
C ₈ H ₁₀ O ₄ (NO ₃) ⁻	232.0463	0.7
C ₇ H ₈ O ₅ (NO ₃) ⁻	234.0255	0.7
C ₈ H ₁₁ O ₉ (NO ₃) ⁻	313.0287	0.7
C ₇ H ₇ O ₄ ⁻	155.0350	0.6

Table A-4595 CI-API-TOF peak list for xylene (C₈H₁₀) oxidation products.

Chemical formula	Mass	Fraction of explained signal
C ₁₆ H ₂₂ O ₈ (NO ₃) ⁻	404.1198	18.0
C ₈ H ₁₂ O ₅ (NO ₃) ⁻	250.0568	12.9
C ₈ H ₁₂ O ₆ (NO ₃) ⁻	266.0518	8.9
C ₈ H ₁₂ O ₇ (NO ₃) ⁻	282.0467	7.6
C ₁₆ H ₂₂ O ₁₀ (NO ₃) ⁻	436.1096	4.3
C ₈ H ₁₄ O ₈ (NO ₃) ⁻	300.0572	3.5
C ₈ H ₁₄ O ₇ (NO ₃) ⁻	284.0623	3.3
C ₁₆ H ₂₂ O ₉ (NO ₃) ⁻	420.1147	2.5
C ₈ H ₁₂ O ₈ (NO ₃) ⁻	298.0416	2.2
C ₁₆ H ₂₂ O ₁₂ (NO ₃) ⁻	468.0995	2.0
C ₈ H ₉ O ₄ ⁻	169.0506	1.7
C ₈ H ₁₂ O ₉ (NO ₃) ⁻	314.0365	1.7
C ₈ H ₁₄ O ₆ (NO ₃) ⁻	268.0674	1.6
C ₁₆ H ₂₄ O ₁₁ (NO ₃) ⁻	454.1202	1.4
C ₈ H ₁₁ O ₆ (NO ₃) ⁻	265.0439	1.4
C ₁₆ H ₂₂ O ₁₁ (NO ₃) ⁻	452.1046	1.2
C ₈ H ₁₀ O ₆ (NO ₃) ⁻	264.0361	1.1
C ₈ H ₁₀ O ₈ (NO ₃) ⁻	296.0259	1.0
C ₁₆ H ₂₄ O ₁₀ (NO ₃) ⁻	438.1253	1.0
C ₈ H ₁₀ O ₅ (NO ₃) ⁻	248.0412	0.9
C ₈ H ₁₃ O ₈ (NO ₃) ⁻	299.0494	0.9
C ₈ H ₁₀ O ₇ (NO ₃) ⁻	280.0310	0.8

Table A-5CI-API-TOF peak list for mesitylene (C₉H₁₂) oxidation products.

Chemical formula	Mass	Fraction of explained signal
C ₁₈ H ₂₆ O ₈ (NO ₃) ⁻	432.1511	24.2
C ₉ H ₁₄ O ₇ (NO ₃) ⁻	296.0623	9.6
C ₉ H ₁₄ O ₆ (NO ₃) ⁻	280.0674	8.2
C ₁₈ H ₂₆ O ₁₀ (NO ₃) ⁻	464.1410	7.0
C ₉ H ₁₆ O ₇ (NO ₃) ⁻	298.0780	4.6
C ₉ H ₁₄ O ₅ (NO ₃) ⁻	264.0725	4.0
C ₉ H ₁₆ O ₈ (NO ₃) ⁻	314.0729	3.3
C ₉ H ₁₆ O ₉ (NO ₃) ⁻	330.0679	3.0
C ₉ H ₁₃ O ₇ (NO ₃) ⁻	295.0545	3.0
C ₉ H ₁₃ O ₆ ⁻	217.0718	2.5
C ₉ H ₁₅ O ₈ (NO ₃) ⁻	313.0651	1.7
C ₁₈ H ₂₆ O ₉ (NO ₃) ⁻	448.1461	1.6
C ₉ H ₁₄ O ₈ (NO ₃) ⁻	312.0572	1.5
C ₉ H ₁₂ O ₆ (NO ₃) ⁻	278.0518	1.5
C ₉ H ₁₇ O ₁₀ (NO ₃) ⁻	347.0705	1.3
C ₉ H ₁₄ O ₁₀ ⁻	282.0592	1.2
C ₉ H ₁₇ O ₉ (NO ₃) ⁻	331.0756	1.2

600

Table A-6CI-API-TOF peak list for naphthalene (C₁₀H₈) oxidation products.

Chemical formula	Mass	Fraction of explained signal
C ₂₀ H ₁₈ O ₄ (NO ₃) ⁻	384.1089	26.1
C ₂₀ H ₁₈ O ₆ (NO ₃) ⁻	416.0987	17.4
C ₂₀ H ₁₈ O ₅ (NO ₃) ⁻	400.1038	4.1
C ₁₀ H ₇ O ₅ ⁻	207.0299	3.5
C ₂₀ H ₁₈ O ₇ (NO ₃) ⁻	432.0936	3.0
C ₂₀ H ₁₈ O ₉ (NO ₃) ⁻	464.0834	2.9
C ₁₀ H ₁₀ O ₄ (NO ₃) ⁻	256.0463	2.5
C ₁₀ H ₁₀ O ₅ (NO ₃) ⁻	272.0412	2.1
C ₁₀ H ₇ O ₃ ⁻	175.0401	1.8
C ₁₀ H ₁₀ O ₈ (NO ₃) ⁻	320.0259	1.7
C ₂₀ H ₁₈ O ₈ (NO ₃) ⁻	448.0885	1.6
C ₁₀ H ₁₀ O ₆ (NO ₃) ⁻	288.0361	1.5
C ₁₀ H ₈ O ₇ (NO ₃) ⁻	302.0154	1.2
C ₂₀ H ₂₀ O ₇ (NO ₃) ⁻	434.1093	1.1
C ₁₀ H ₇ O ₄ ⁻	191.0350	1.0
C ₂₀ H ₁₈ O ₁₀ (NO ₃) ⁻	480.0784	1.0
C ₂₀ H ₁₈ O ₁₁ (NO ₃) ⁻	496.0733	1.0
C ₁₀ H ₁₂ O ₆ (NO ₃) ⁻	290.0518	0.9
C ₁₀ H ₁₀ O ₇ (NO ₃) ⁻	304.0310	0.9
C ₁₀ H ₇ O ₆ ⁻	223.0248	0.9
C ₁₀ H ₇ O ₇ ⁻	239.0197	0.9
C ₁₀ H ₈ O ₅ (NO ₃) ⁻	270.0255	0.9
C ₁₀ H ₁₀ O ₁₀ (NO ₃) ⁻	352.0158	0.8
C ₁₀ H ₁₀ O ₉ (NO ₃) ⁻	336.0208	0.6

Table A-7CI-API-TOF peak list for biphenyl (C₁₂H₁₀) oxidation products.

Chemical formula	Mass	Fraction of explained signal
C ₂₄ H ₂₂ O ₈ (NO ₃) ⁻	500.1198	9.1
C ₁₂ H ₁₂ O ₅ (NO ₃) ⁻	298.0569	6.2
C ₁₂ H ₁₄ O ₆ (NO ₃) ⁻	316.0674	5.6
C ₂₄ H ₂₂ O ₇ (NO ₃) ⁻	484.1249	4.9
C ₂₄ H ₂₄ O ₇ (NO ₃) ⁻	486.1406	3.7
C ₁₂ H ₉ O ₄ ⁻	217.0506	3.6
C ₁₂ H ₉ O ₃ ⁻	201.0557	3.5
C ₂₄ H ₂₂ O ₆ (NO ₃) ⁻	468.1300	3.5
C ₂₄ H ₂₂ O ₉ (NO ₃) ⁻	516.1147	3.2
C ₂₄ H ₂₄ O ₉ (NO ₃) ⁻	518.1304	2.9
C ₂₄ H ₂₄ O ₈ (NO ₃) ⁻	502.1355	2.8
C ₂₄ H ₂₂ O ₁₁ (NO ₃) ⁻	548.1046	2.5
C ₁₂ H ₁₂ O ₆ (NO ₃) ⁻	314.0518	2.4
C ₁₂ H ₁₂ O ₈ (NO ₃) ⁻	346.0416	2.3
C ₁₂ H ₁₄ O ₅ (NO ₃) ⁻	300.0725	1.7
C ₁₂ H ₁₄ O ₇ (NO ₃) ⁻	332.0623	1.7
C ₁₂ H ₁₂ O ₇ (NO ₃) ⁻	330.0467	1.4
C ₂₄ H ₂₂ O ₁₀ (NO ₃) ⁻	532.1097	1.4
C ₁₂ H ₁₂ O ₉ (NO ₃) ⁻	362.0365	1.4
C ₁₁ H ₉ O ₃ ⁻	189.0557	1.4
C ₁₂ H ₉ O ₅ ⁻	233.0455	1.2
C ₁₂ H ₁₀ O ₄ ⁻	218.0585	1.1
C ₂₄ H ₂₄ O ₁₀ (NO ₃) ⁻	534.1253	1.1
C ₂₄ H ₂₄ O ₅ (NO ₃) ⁻	454.1507	1.1
C ₂₄ H ₂₂ O ₁₂ (NO ₃) ⁻	564.0995	1.1
C ₂₄ H ₂₁ O ₈ ⁻	437.1242	1.0
C ₁₂ H ₁₂ O ₄ (NO ₃) ⁻	282.0619	1.0
C ₁₂ H ₁₁ O ₄ ⁻	219.0663	1.0
C ₁₀ H ₉ O ₂ ⁻	161.0608	0.8
C ₁₂ H ₁₀ O ₂ (NO ₃) ⁻	248.0564	0.8
C ₃₆ H ₃₄ O ₁₀ (NO ₃) ⁻	688.2036	0.8
C ₁₂ H ₁₁ O ₅ ⁻	235.0612	0.7
C ₁₂ H ₁₀ O ₄ (NO ₃) ⁻	280.0463	0.7
C ₁₁ H ₇ O ₂ ⁻	171.0452	0.7
C ₂₄ H ₂₂ O ₅ (NO ₃) ⁻	452.1351	0.6
C ₁₀ H ₇ O ₃ ⁻	175.0401	0.6
C ₁₀ H ₇ O ₄ ⁻	191.0350	0.6

610 **Appendix B**

HOMs from the 7 tested compounds are presented in the next figures. Top panel left: pie chart showing the monomer and dimer fraction; 3 bar plots presenting the relative signal intensities for radicals, monomer and dimers. In the bar plots, the x axis presents the number of oxygen atoms and the colour code the number of hydrogen atoms for each of the HOMs.

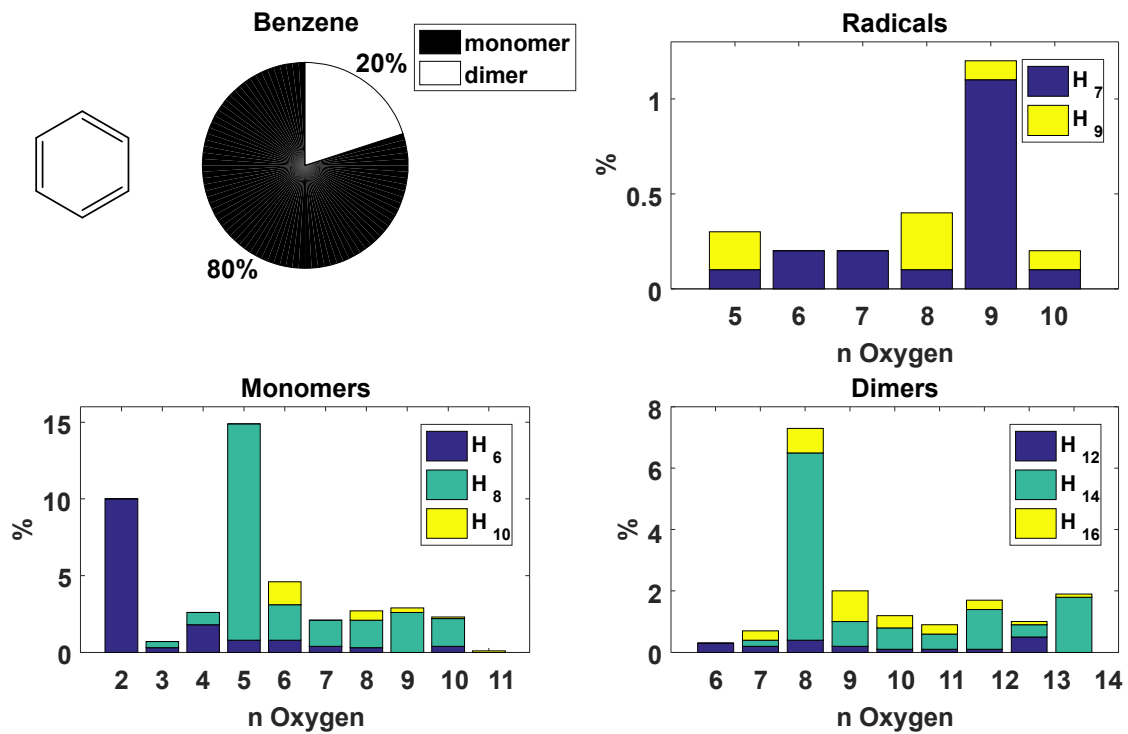


Figure B – 1 Benzene

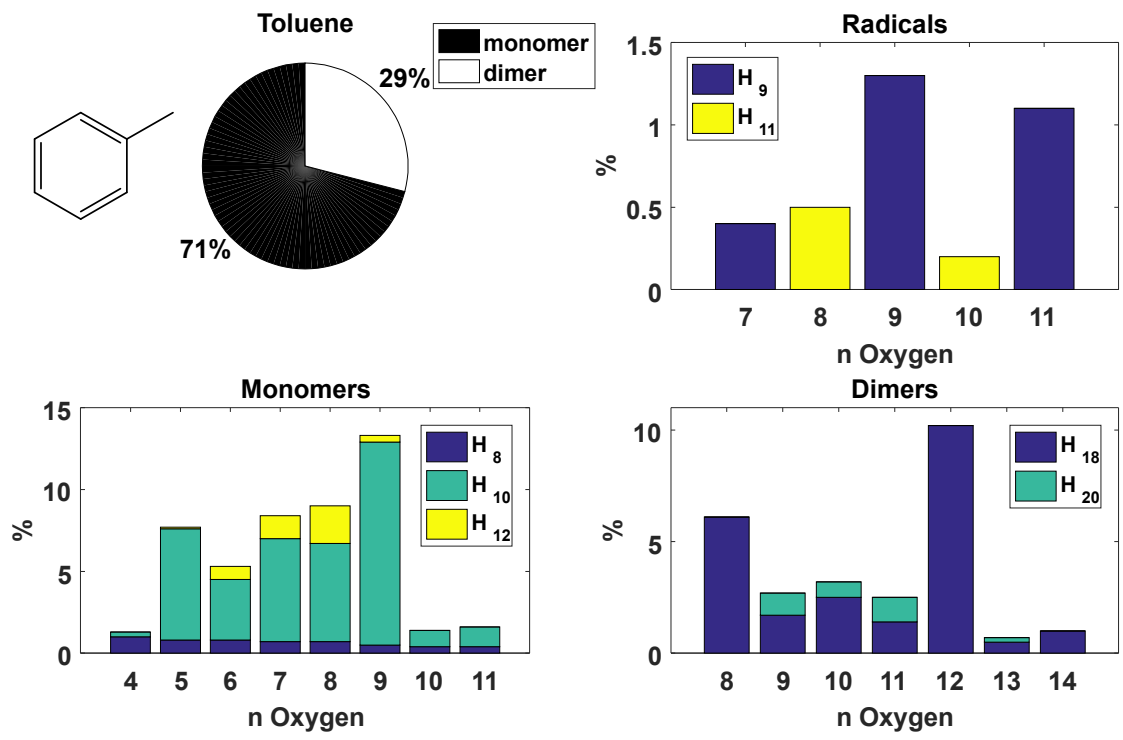


Figure B – 2 Toluene

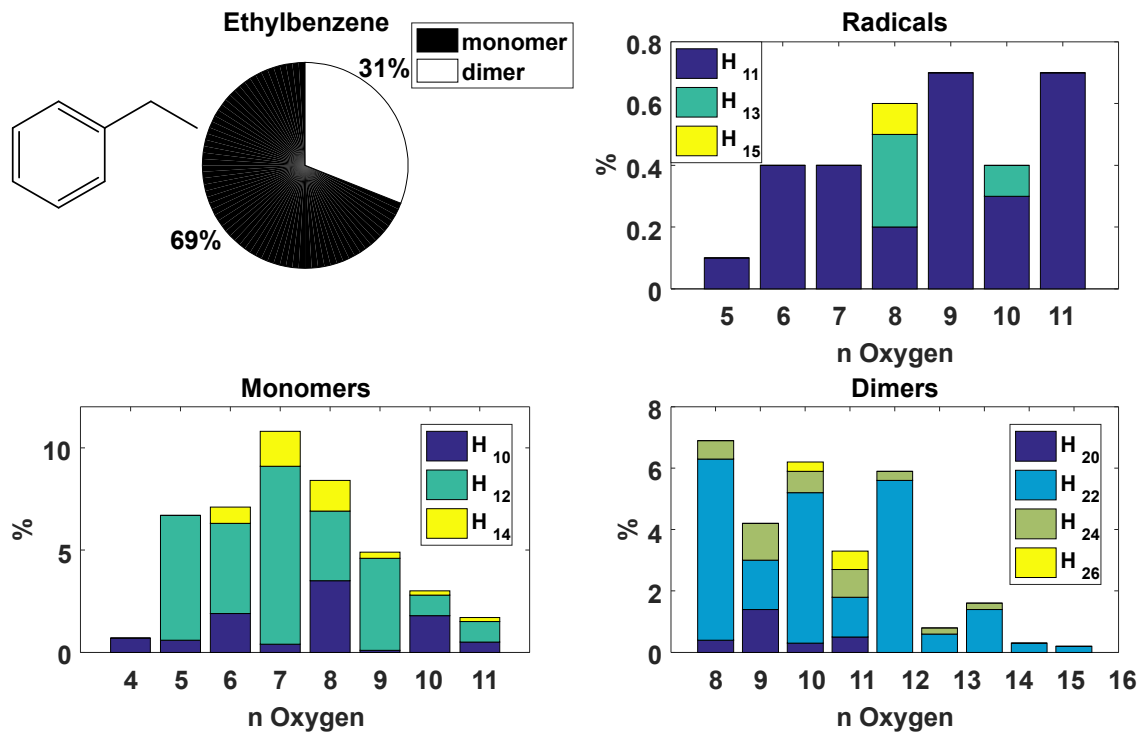
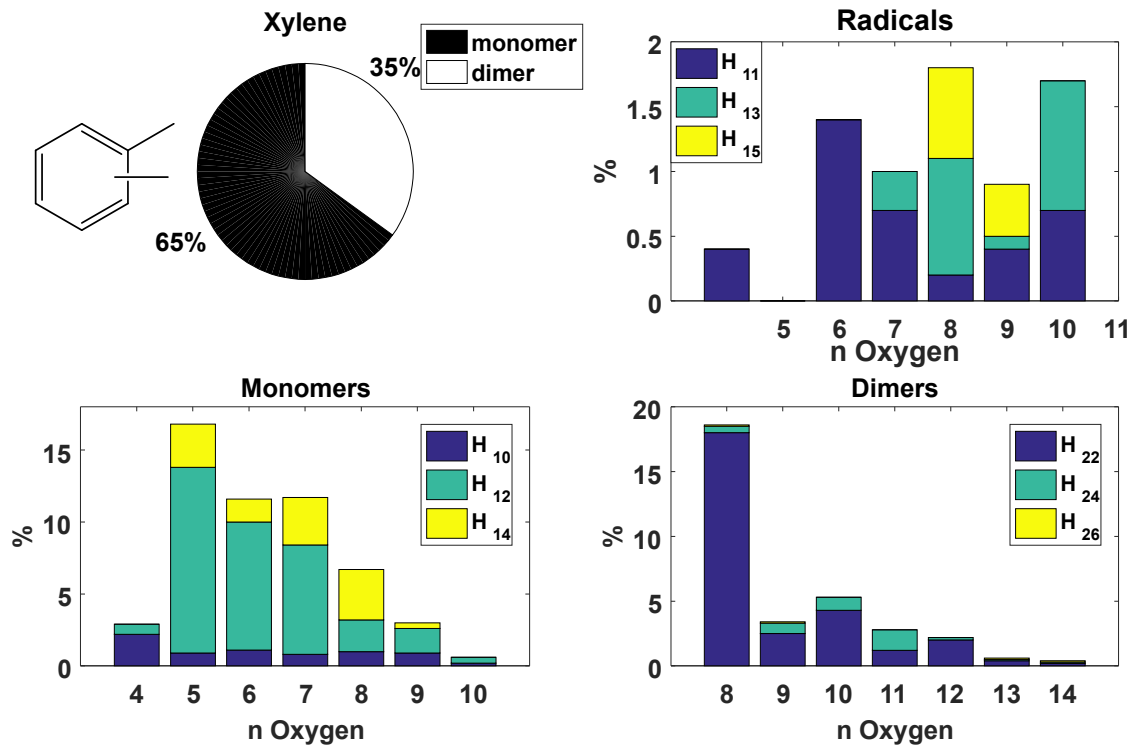
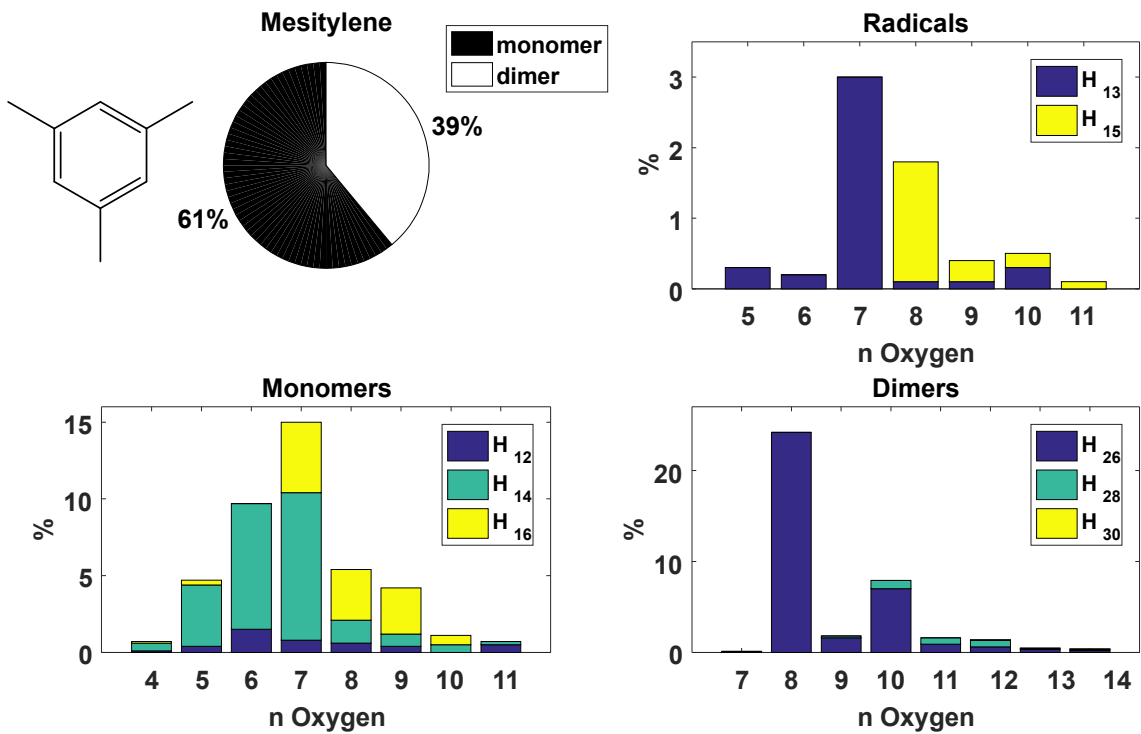


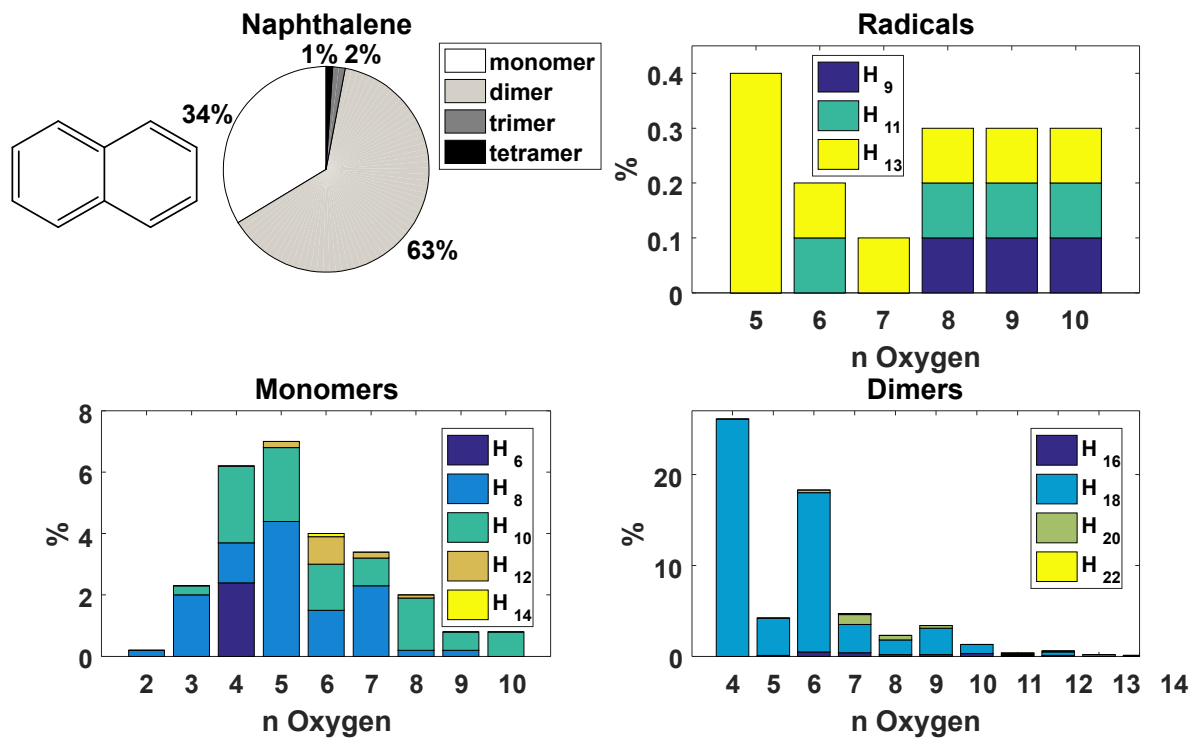
Figure B – 3 Ethylbenzene



625 | Figure B – 4 Xylene



| Figure B – 5 Mesitylene



630 Figure B – 6 Naphthalene

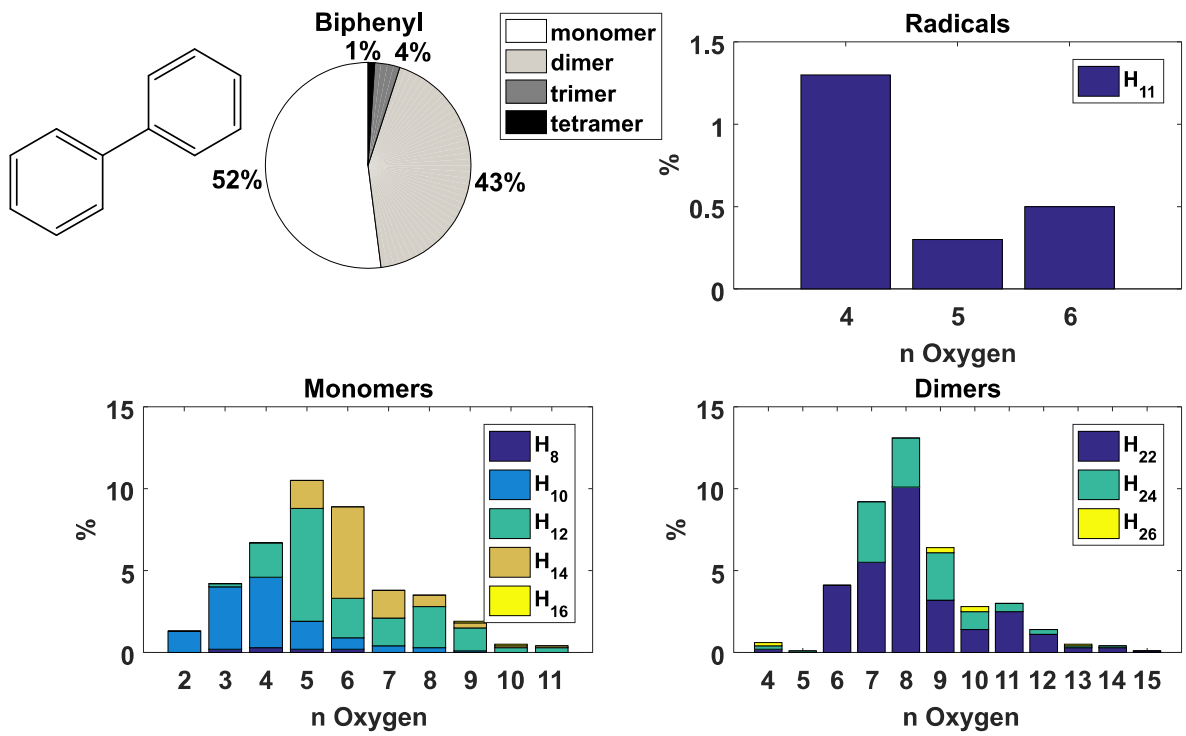


Figure B – 7 Biphennyl

Appendix C

635 The radiation at 172 nm excites molecular oxygen and water vapor triggering the following radical reactions:



The humidified air flow is exposed to the 172 nm radiation for 50 ms and is then within 30 ms transferred to the mixing zone with the sample flow. The oxidant species produced are OH, HO₂, O₃ and H₂O₂. The final OH concentration entering the mixing zone depends on the residence time in the lamp and in the transfer region.

640

The kinetic model includes 31 species and 36 reactions from the MCM 3.3.1 (Jenkin et al., 2003). Mesitylene is selected as ArHC for these simulations and its reaction mechanism is extended up to the second generation products. The model is run for 20 seconds in agreement with the residence time of the flow tube reactor with a simulation time resolution of 2 ms. The model is initiated with the measured concentrations of ozone (3.45 10¹² molecules cm⁻³ without mesitylene) and mesitylene (2.46 10¹² molecules cm⁻³ without lamp on) at the exit of the flow tube. The initial OH radical concentration (8.50 10¹¹ molecules cm⁻³) is tuned in order to match the OH exposure, which was determined from the amount of reacted mesitylene. The initial HO₂ radical concentration (1.70 10¹² molecules cm⁻³) is set at twice the initial OH radical concentration. Wall losses of about 35% are estimated for mesitylene HOMs but are not implemented in the model. Figure C1 shows the temporal evolution of 6 selected species: reacted mesitylene (TM135MB reacted), HO₂ radical (HO2), OH radical (OH) as well as 3 products of the mesitylene oxidation with the OH radical (TM135BPRO2, TM135BPOOH and TM135B2OH). TM135BPRO2 is an intermediate peroxy radical after OH attack; TM135BPOOH is a product from the reaction of TM135BPRO2 with the HO₂ radical while TM135BPO2OH is a product from the reaction of TM135BPRO2 with a peroxy radical RO₂. Mesitylene reacted reaches a plateau after about 0.03 seconds while TM135BPRO2 reaches a maximum value around 0.01-0.02 seconds and then rapidly decreases. The closed shell products TM135BPOOH and TM135BPO2OH constantly increase and reach a plateau after about 0.4-1.0 seconds. A similar trend could be expected for HOMs assuming that TM135BPRO2 undergoes an autoxidation chain and is terminated either by HO₂ or by RO₂. In a test run where the initial mesitylene concentration and the reaction rate constant towards OH radicals were doubled, the ratio TM135BPOOH/TM135BPO2OH varied only by about 18%.

650

655

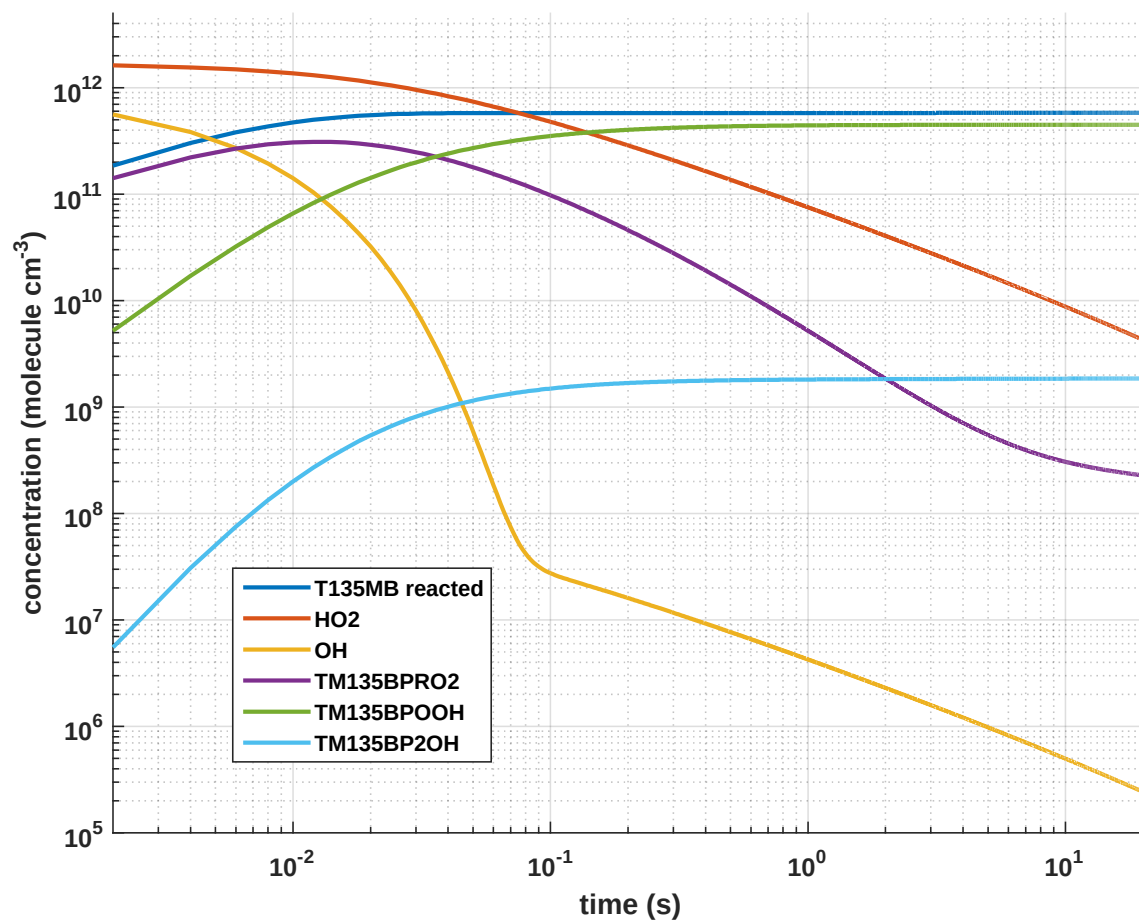


Figure C1. Temporal evolution of selected species according to the mesitylene flow tube kinetic model.

Author's response:

We thank the Referees for the careful revision and comments, which helped improving the overall quality of the manuscript.

A point-by-point answer to the referees' remarks is detailed in the following (in black the referee comments, in blue our answers, in green text modifications)

Referee #1

The authors describe experimental findings from a flow-tube study on HOM formation from the reaction of OH radicals with a series of aromatic compounds. OH radicals were generated by water VUV photolysis at 172 nm. The OH+aromatic reaction carried out in a flow system was separated from the OH radical production. Nitrate CIMS was chosen for HOM detection. OH radical concentrations in the system were obtained using an indirect way via a scavenger method. HOM formation from aromatic compounds represents an interesting topic within the framework of SOA precursor formation. It could be a very important process for SOA formation in urban areas. This manuscript needs a couple of clarifications and further explanations before publication can be recommended. Here my comments:

Line 17: From my perspective, the authors do not present “identified products”, they simply show product signals and they discuss possible moieties or structural elements of these products.

We agree that not the chemical structures but only the molecular formulas of the HOMs were identified. We modified the text accordingly:

We report the elemental composition of the HOMs and show the differences in the oxidation patterns of these ArHCs.

Line 48: It is better to say: “aromaticity is lost (or is abrogated)”

We agree and we modified this:

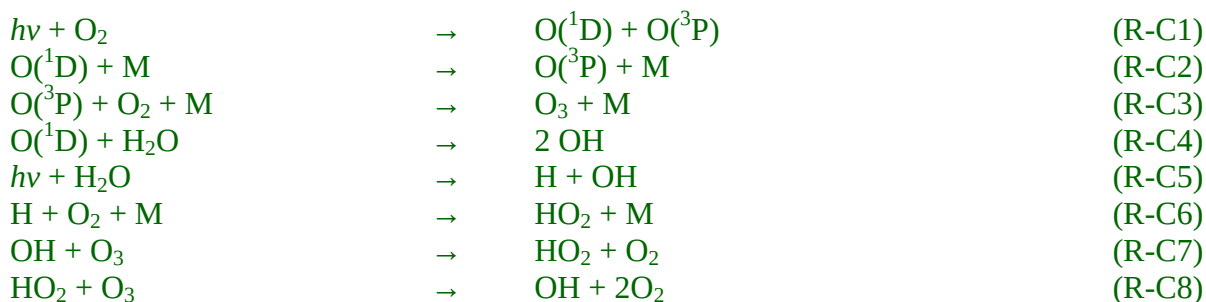
When the aromaticity is lost by the OH addition, non-aromatic double bonds are ...

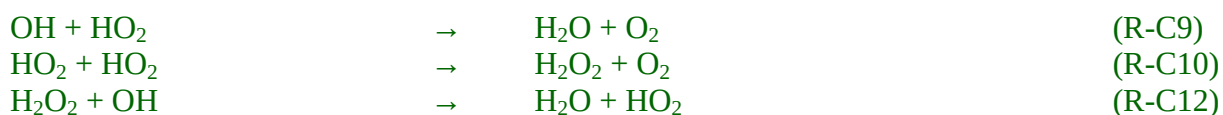
Line 65: OH radicals were generated by water photolysis using a Xe excimer lamp. The atmospheric chemistry community does not commonly use this approach of OH formation. It should be explained here more in detail what are the main reaction steps in a water/air mixture after irradiation at 172 nm. I guess it is also important to comment on the formation of other products like HO₂, H₂O₂ and ozone and their concentration levels in the reaction gas. How important is especially the reaction of OH radicals with HO₂ before entering the mixing zone with the flow containing the aromatic compound? It is not enough to state some references only.

We include in the appendix section (Appendix C) a description of the OH radical formation with the Xe excimer lamp and a model of the chemistry in these experiments.

Appendix C

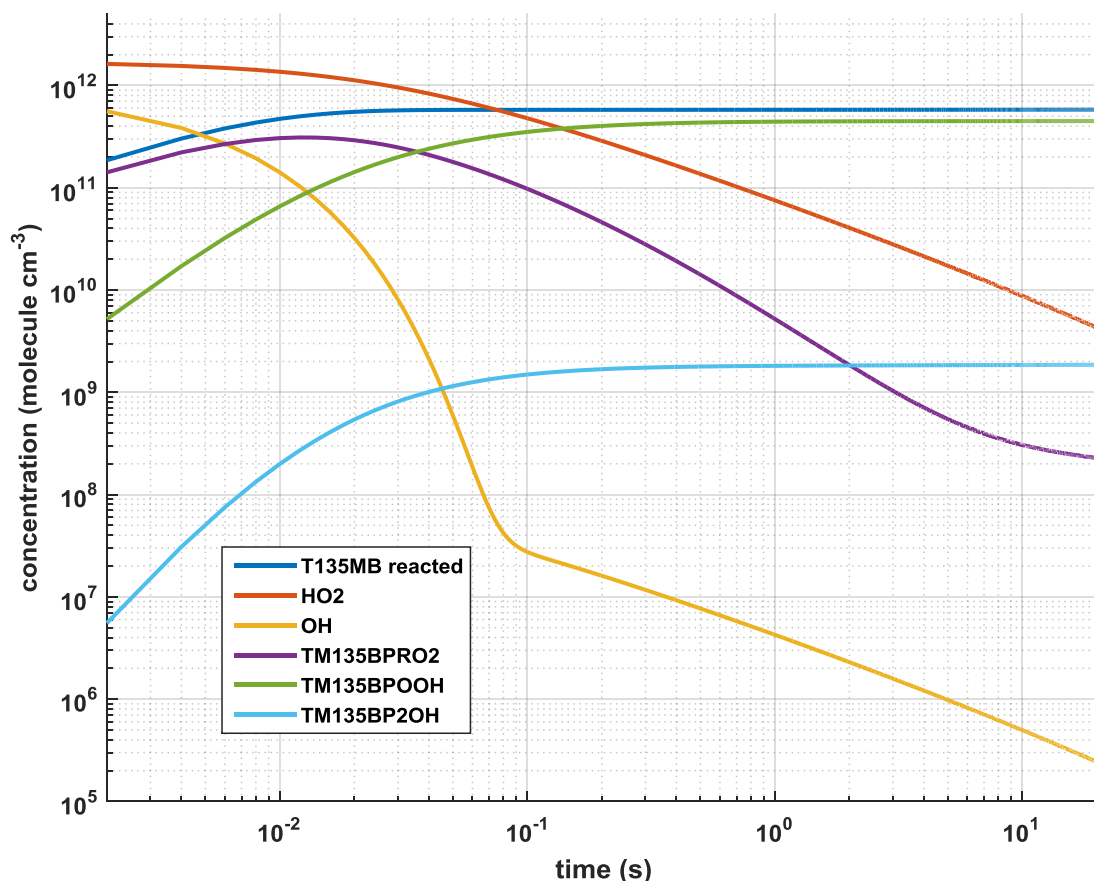
The radiation at 172 nm excites molecular oxygen and water vapor triggering the following radical reactions:





The humidified air flow is exposed to the 172 nm radiation for 50 ms and is then within 30 ms transferred to the mixing zone with the sample flow. The oxidant species produced are OH, HO₂, O₃ and H₂O₂. The final OH concentration entering the mixing zone depends on the residence time in the lamp and in the transfer region.

The kinetic model includes 31 species and 36 reactions from the MCM 3.3.1 (Jenkin et al., 2003). Mesitylene is selected as ArHC for these simulations and its reaction mechanism is extended up to the second generation products. The model is run for 20 seconds in agreement with the residence time of the flow tube reactor with a simulation time resolution of 2 ms. The model is initiated with the measured concentrations of ozone ($3.45 \cdot 10^{12}$ molecules cm⁻³ without mesitylene) and mesitylene ($2.46 \cdot 10^{12}$ molecules cm⁻³ without lamp on) at the exit of the flow tube. The initial OH radical concentration ($8.50 \cdot 10^{11}$ molecules cm⁻³) is tuned in order to match the OH exposure, which was determined from the amount of reacted mesitylene. The initial HO₂ radical concentration ($1.70 \cdot 10^{12}$ molecules cm⁻³) is set at twice the initial OH radical concentration. Wall losses of about 35% are estimated for mesitylene HOMs but are not implemented in the model. Figure C1 shows the temporal evolution of 6 selected species: reacted mesitylene (T135MB reacted), HO₂ radical (HO2), OH radical (OH) as well as 3 products of the mesitylene oxidation with the OH radical (TM135BPRO2, TM135BPOOH and TM135BPO2OH). TM135BPRO2 is an intermediate peroxy radical after OH attack; TM135BPOOH is a product from the reaction of TM135BPRO2 with the HO₂ radical while TM135BPO2OH is a product from the reaction of TM135BPRO2 with a peroxy radical RO₂. Mesitylene reacted reaches a plateau after about 0.03 seconds while TM135BPRO2 reaches a maximum value around 0.01-0.02 seconds and then rapidly decreases. The closed shell products TM135BPOOH and TM135BPO2OH constantly increase and reach a plateau after about 0.4-1.0 seconds. A similar trend could be expected for HOMs assuming that TM135BPRO2 undergoes an autoxidation chain and is terminated either by HO₂ or by RO₂. In a test run where the initial mesitylene concentration and the reaction rate constant towards OH radicals were doubled, the ratio TM135BPOOH/TM135BPO2OH varied only by about 18%.



Line 81: Obviously, the reagent ion spectrum showed a strong signal of trifluoroacetate arising from fluorinated contaminants of the Nafion membrane. Was there also a strong signal of the “dimer”, i.e. the trifluoroacetate adduct with trifluoroacetic acid? It would be fine to see a reagent ion spectrum as recorded for commonly used reaction conditions (maybe in Appendix). Was the trifluoroacetate concentration low enough that a possible contribution in the ionization process can be excluded?

The main source of trifluoroacetate is indeed the Nafion membrane. Additional experiments (not presented here) with a bubbler showed a much lower trifluoroacetate signal. The trifluoroacetate monomer was the main peak followed by the adduct with nitric acid and the trifluoroacetate dimer. In the experiments where the trifluoroacetate signal was rather high we did not observe adducts with HOMs. From this we conclude that trifluoroacetate did not influence the ionization of the analyte.

Line 84: What was the procedure applied for the determination of the “average” OH radical concentration? Was the disappearance of deuterated butanol monitored by PTR-MS when OH formation was switched on? What was the initial butanol concentration? I guess it has been done in absence of the aromatics, or not? The authors used a kind of a discharge technique. Consequently, the initial OH concentration was much higher than the “average” concentration of 1.9×10^8 molec./cc.? Please provide more information. In addition, the authors could show a figure with OH, aromatic and total HOM concentrations as a function of time or reactor length

The OH concentration was determined from the difference in precursor concentration between excimer lamp switched on or off. Two D9-butanol, toluene, mesitylene, and biphenyl experiments resulted in an average value of 2×10^8 OH radicals cm⁻³. It was not possible to derive an OH

concentration from the benzene, ethylbenzene and naphthalene experiments due to technical difficulties. As xylene was a mixture of 3 isomers with different OH-reaction rate constants, the OH concentration could not be determined. We assume that the OH production was constant in all experiments as the lamp was operated under similar conditions. We developed a kinetic model to simulate the decrease of the aromatic compounds under the conditions of our flow tube experiments. This is described in the appendix (Appendix section C), which includes a figure with the concentrations of OH, aromatic precursor and a HOM representative as a function of time (see description above).

Line 92: At this point it is not clear where the (molar?) HOM formation yields are coming from? Did the authors measure the disappearance of the aromatics by PTRMS, if measurable? Or did the authors calculate the amount of converted aromatics based on their measured OH radical concentration? The concentrations of converted aromatics along with the total HOM concentrations should be stated in Table 1 or in a separate table. What was the calibration factor used for the HOM concentrations measured by nitrate CIMS, where does it come from and what is the detection limit for these HOMs? Please clarify the way of concentration determination for reacted aromatics as well as for the HOMs.

The HOM molar yield was calculated from the ratio of HOM concentration to reacted ArHC (the yields were not corrected for the HOMs losses). The amount of ArHC reacted was calculated based on the assumption, that the OH production was similar in all experiments (see comment above). The HOMs quantification is based on the calibration factor for sulfuric acid and the assumption that HOMs have the same ionization efficiency as sulfuric acid (Ehn et al., 2014; Kirkby et al., 2016). It is known that the ionization efficiency depends on the structure of the HOMs. Since the ionization efficiency might be <1 for some HOM structures, the reported concentrations here represent lower limits. We added the following in the text:

HOMs yields are calculated as the ratio of HOMs measured to ArHC reacted. HOMs were quantified using the calibration factor for sulfuric acid and assuming the same charging efficiency for HOMs (Ehn et al., 2014; Kirkby et al., 2016). From the decrease of the precursor concentration (lights off versus lights on) we determined an average OH concentration. From the experiments with D9-butanol, toluene, mesitylene and biphenyl an average OH concentration of $2 \cdot 10^8 \text{ OH cm}^{-3}$ was obtained. Assuming the same OH production of the lamp in all experiments ArHC reacted was calculated from the OH radical exposure using the reaction rate coefficients at 25°C.

Table 1 was complemented with HOMs concentration, reacted fraction of ArHCs and HOMs yield and looks now like this:

Table 1

Initial concentrations of precursors, reaction rate coefficients, ArHC reacted fraction (%), total HOMs concentration and HOMs yield (%). The mixing ratio of precursors was determined at the exit of the flow tube when the excimer lamp (OH generation) was switched off.

Compound	Concentration (molecules cm^{-3})	k_{OH} ($10^{-12} \text{ cm}^3 \text{ molecules}^{-1} \text{ s}^{-1}$)	Reacted fraction (%)	[HOM] (molecules cm^{-3})	HOMs yield (%)
Benzene (C_6H_6)	$9.85 \cdot 10^{13}$	1.22	0.5	$1.2 \cdot 10^9$	0.2
Toluene (C_7H_8)	$1.97 \cdot 10^{13}$	5.63	2.3	$4.4 \cdot 10^8$	0.1
Ethylbenzene (C_8H_{10})	$1.13 \cdot 10^{13}$	7.0	2.8	$9.4 \cdot 10^8$	0.3

(o/m/p)-xylene (C ₈ H ₁₀)	2.95 10 ¹²	13.6/23.1/14.3	//	2.8 10 ⁹	//
Mesitylene (C ₉ H ₁₂)	2.46 10 ¹²	56.7	22.7	3.1 10 ⁹	0.6
Naphthalene (C ₁₀ H ₈)	2.95 10 ¹³	23.0	9.2	1.4 10 ¹⁰	0.5
Biphenyl (C ₁₂ H ₁₀)	4.43 10 ¹³	7.1	2.8	1.8 10 ¹⁰	1.4

Reference for the *k*-rates: (Atkinson and Arey, 2003)

Line 95 and Fig.2: Main peaks in Fig.2 should be numbered and this numbering should be also given in the corresponding signal table in Appendix. It makes it easier to understand the signal assignment.

We updated Figure 2 by adding for each compound the chemical structure on the left side of the figure. To help the reader we included labels with the oxygen number in the monomer and dimer panels.

See Figure 2.

Line 110 and Table 2: The detected product distribution is strongly dependent on the reaction conditions and, therefore, only valid for the conditions of this experiment. That should be clearly mentioned at this point.

We agree with this. The new text reads:

However, since the mass-dependent ion transmission efficiency is rather smooth the given values may faithfully represent the relative product distribution of the different aromatic compounds.

Line 124: What does it mean “more oxygenated radicals have a higher probability to undergo an auto-termination radical reaction”? Please state this pathway and give more information for that.

This statement can be derived from (Rissanen et al., 2014): We rewrote it as follows:

Additionally, more oxygenated radicals have a higher probability to undergo a unimolecular termination compared to a radical-radical recombination (RO₂· + RO₂· or RO₂· + HO₂·). More oxygen atoms imply more peroxy functional groups and therefore a higher probability of a hydrogen abstraction in geminal position of a peroxide which results in an OH radical loss and a carbonyl group formation.

Line 161: Do the authors believe that they are able to detect RO radicals by nitrate CIMS? What is the expected RO lifetime with respect to isomerization and for a possible reaction with O₂ (depending on the structure)?

We do not detect alkoxy radicals. Based on our understanding their lifetime is too short to yield detectable concentrations. From the fact that compounds with even numbers of oxygen are observed we infer that the alkoxy radical isomerizes to a carbon centered radical and takes up oxygen molecules in an auto-oxidation mechanism. This is explained in the text in the lines 166-168.

Line 167: “uptake an oxygen atom”?

We replaced atom with molecule.

can again take up an oxygen molecule.

Line 223: At the end of this paragraph a discussion on possible ozone reactions of products is welcome. The ozone concentration in this experiment is quite high and the products have to

contain double bonds after losing the aromaticity. Moreover, a statement is needed how the results of this study can be used to explain the formation of SOA precursors for urban conditions where the reaction of RO₂+NO dominates the RO₂ fate in most cases.

While the ArHC do not react with ozone, oxidation products with remaining double bonds indeed may. The ozone concentration produced in the Xe excimer lamp is about 140 ppb. The residence time in the flow tube is 20 s. Reaction rate constants for the ozonolysis of alkenes are in the range of $10^{-16} - 10^{-18} \text{ cm}^3 \text{ molecule}^{-1} \text{ s}^{-1}$. Under the condition that 20 ppb of ArHC have reacted and yield 10% of products with a double bond still containing the carbon skeleton of the parent molecule, about 0.14 - 14 ppt of these products will react with ozone. Assuming a high HOMs yield of 10% from this ozonolysis reaction we can expect 0.014-1.4 ppt of HOMs from ozonolysis. This can be compared to 60-800 ppt HOMs produced via OH radical attack. Thus, the contribution of ozonolysis to HOMs formation can be neglected.

We added the following to the text:

Under urban conditions, in the presence of NO, the reaction of RO₂+NO will compete with the autoxidation pathway. This can lead to relatively highly oxygenated nitrates of low volatility or oxyradicals. The latter can isomerize to a carbon centered radical as under our conditions and again undergo autoxidation. Highly oxygenated organic nitrates have been recently identified in SOA (Lee et al., 2016). While this study shows that autoxidation can also occur after an OH attack of ArHC, the formation of low volatility products via this route in the presence of NO, which is typical of urban atmospheres, needs further investigation.

First generation oxidation products may still contain carbon-carbon double bonds, which could also further react with ozone forming more highly oxygenated products. Since the reaction time is very short in the flow tube this reaction is negligible but could be another potential pathway in the ambient atmosphere.

Fig.5: What does “Product with DB” mean?

DB means products with double bonds.

This is now mentioned in Figure 5.

Referee #2

Significance This is an interesting work describing the important observation of highly oxidized molecules (HOM) from aromatic oxidation reactions. Although certainly important observation in a current “hot-topic” field, and as such should merit its publication, I have a problem how the results are presented. It almost seems as this has been written with a format more suitable for general wider audience in a magazine format, and not really addressed to the atmospheric chemist and physics community. I feel that a certain amount of details of the experiments and the setup have been omitted, which could greatly help researchers in the field performing these type of experiments. Due to this formatting issue in many cases it seems that the text just assumes too much from the reader. This will become clearer from the large amount of specific comments given below and starting with: “What do you mean by..”. So while I find the topic extremely interesting and the finding important, I cannot recommend publication in the current form. I further stress that most of this is due to the current presentation form and all of the problems can be fixed relatively easily. Thus I strongly suggest that the authors take time to modify/rewrite the text according to the comments given below, after which I can recommend publishing.

Major Comments:

Abstract should contain the major details of the work described in the manuscript, i.e., what was studied with what methods and what were the main results, and Conclusions should contain summary of the results and their significance. At the moment they do not do this. More precisely, currently Abstract is missing many of these details and Conclusions feels more like an extension of Discussion. I suggest significantly improving the current presentation.

We have modified Abstract and Conclusions accordingly

In the Abstract you talk about identified compounds, although there were no single compound really identified in the whole study. This should be changed.

Referee #1 has raised a similar comment. We agree and modified the sentence to:

We report the molecular formulas of the HOMs and show the differences in the oxidation patterns of these ArHCs.

In the Abstract you talk about mechanistic pathways – was there more than the one shown for mesitylene in Figure 6?

We show a possible oxidation pathway for mesitylene as an example case. The other single ring aromatics may follow a similar scheme, although branching ratios may vary. We now say:

A potential pathway for the formation of these HOMs from aromatics is presented and discussed.

Also in line 53 you say that you talk about “potential pathways and possible mechanism”, but I feel that currently the mechanistic aspects are only briefly discussed.

Indeed, the lack of unambiguous identification of molecular structures does not allow for an extensive evaluation of the mechanism. We present a generalized scheme of a mechanism, which represents the observed elemental composition of species, and discuss a potential pathway of HOMs formation. We changed the wording such that it should be clear that we do not provide proofs of a detailed mechanism. The sentence reads now:

Here we show the formation of HOMs from ArHC upon reaction with OH radicals. We present product distributions of HOMs in terms of molecular masses and molecular formulas for a series of aromatic precursors based on measurements with a nitrate chemical ionization atmospheric pressure interface time of flight mass spectrometer (CI-APi-TOF) (Ehn et al., 2014; Jokinen et al., 2012; Kürten et al., 2011). A potential pathway along with a possible mechanism for the formation of HOMs from aromatic compounds is discussed.

More details of the OH radical production, especially the geometry and the distance OH needs to travel, could be helpful. It was stated that this setup has been used to generate HO₂, which is co-produced by H₂O photolysis in presence of O₂, but HO₂ is much less reactive and thus can travel much further, whereas OH is easily lost to impurities and walls (and as far as I understood OH needs to travel through two 90 degree bends, from which at least the other is a turbulent zone?). Was there only one experiment with one hydrocarbon?

The humidified air flow is exposed to the 172 nm radiation for 50 ms and is then within 30 ms transferred to the mixing zone with the sample flow. The oxidant species entering the mixing zone are OH, HO₂, O₃ and H₂O₂. Their concentrations depend on the residence time in the lamp and the reaction time in the transfer region. This is now explained in Appendix C together with the chemical reactions forming the oxidants. Despite potentially higher losses of OH to the walls compared to HO₂, there was still enough OH present to react with the precursor gases. The same setup was used for all precursors and for D9-butanol. From this we derived an initial OH concentration of about $8.5 \cdot 10^{11} \text{ cm}^{-3}$.

See Appendix C.

Was the OH production always exactly the same? These should be stated clearly.

The OH concentration was determined from the difference in precursor concentration between excimer lamp switched on or off. Two D9-butanol, toluene, mesitylene, and biphenyl experiments resulted in an average value of $2 \cdot 10^8 \text{ OH radicals cm}^{-3}$. It was not possible to derive an OH concentration from the benzene, ethylbenzene and naphthalene experiments due to technical difficulties. As xylene was a mixture of 3 isomers with different OH-reaction rate constants, the OH concentration could not be determined. We assume that the OH production was constant in all experiments as the lamp was operated under similar conditions.

From the decrease of the precursor concentration (lights off versus lights on) we determined an average OH concentration. From the experiments with D9-butanol, toluene, mesitylene and biphenyl an average OH concentration of $2 \cdot 10^8 \text{ OH cm}^{-3}$ was obtained. Assuming the same OH production of the lamp in all experiments ArHC reacted was calculated from the OH radical exposure using the reaction rate coefficients at 25°C.

It would be very helpful to give the precursor structures to help the reader understand the significance of these oxidation processes.

The chemical structures of the precursors are now included in Figure 2.

Line 84: Could you include a figure showing the process of OH concentration determination as it is very central to the whole topic.

An average OH concentration was determined from the decrease of the precursor gases with the lamp off and on. Using a kinetic model we derived the initial OH concentration and the profile of the precursors. This is now provided in Appendix C.

Line 86: You talk about reactive non-aromatic double bonds together with 140 ppbv ozone – how is it “expected” that O₃ reactions do not play a role here?

This question was also raised by referee #1.

While the ArHC do not react with ozone, oxidation products with remaining double bonds indeed do. The ozone concentration produced in the Xe excimer lamp is about 140 ppb. The residence time in the flow tube is 20 s. Reaction rate constants for the ozonolysis of alkenes are in the range of $10^{16} - 10^{18} \text{ cm}^3 \text{ molecule}^{-1} \text{ s}^{-1}$. Under the condition that 20 ppb of ArHC have reacted and yield 10% of products with a double bond still containing the carbon skeleton of the parent molecule, about 0.14 - 14 ppt of these products will react with ozone. Assuming a high HOMs yield of 10% from this ozonolysis reaction we can expect 0.014-1.4 ppt of HOMs from ozonolysis. This can be compared to 60-800 ppt HOMs produced via OH radical attack. Thus, the contribution of ozonolysis to HOMs formation can be neglected.

Line 112: Would you expect the dimer/monomer ratio to be constant? If, then why so? This should be stated. Furthermore, what do you mean by this being a good proxy? How and why?

We do not expect the dimer to monomer ratio to be the same for all precursors. Indeed the ratios might be somewhat different when measured with different instruments because the transmission functions are not the same. Since the transmission of ions may vary with the voltage settings in the two quadrupoles in the APi, dimer:monomer ratios may differ between instruments. However, since the transmission curve is expected to be rather smooth the relative trend of the dimer/monomer within the 5 single-ring ArHC may still be reasonably accurate due to the small mass differences in the monomer and dimer ranges. We modified the sentence:

However, since the mass-dependent ion transmission efficiency is rather smooth the given values may faithfully represent the relative behavior of the product distribution of the different aromatic compounds.

Line 117: How much of the given abundancies could be actually due to shifting transmission of the mass spec? Is this a potential problem?

As commented above this should have a small effect on the relative changes of the monomer:dimer ratio. This could be a problem if the instrument were tuned in such a way that the ion transmission is strongly mass dependent. Usually, one tries to avoid this.

Line 118: I guess this also assumes that the $k(\text{RO}_2 + \text{HO}_2)$ is similar for all systems? Should be stated. Moreover, according to Table 1 different VOC concentrations were used (which have different rate coefficients with OH), which leads to different $[\text{RO}_2]$ and to different strength of $\text{RO}_2 + \text{RO}_2$, right?

Yes, we assume a similar $k(\text{RO}_2 + \text{HO}_2)$. We think it is a reasonable assumption that the reaction rate $\text{RO}_2 + \text{HO}_2$ does vary less with different substituents compared to the reaction of RO_2 with RO_2 . The master chemical mechanism also uses just one rate constant for this reaction.

The lamp produces a similar concentration of OH and HO_2 in all experiments independent of the precursor concentration. This means that the concentration of RO_2 produced and the amount of HO_2 present is similar in the different experiments. In our sensitivity test with the flow tube kinetic model for mesitylene we selected the species TM135BPOOH and TM135BP2OH as proxy for products of $\text{RO}_2\text{-HO}_2$ and $\text{RO}_2\text{-RO}_2$ reactions. When the initial mesitylene concentration and the reaction rate coefficient with the OH radical were doubled the ratio TM135BPOOH / TM135BP2OH changed only by 18%. Therefore we believe that the observed differences among the tested ArHC compounds can be attributed to a different selectivity rather than to a different radical concentration. We changed the text to:

This indicates that the branching ratio of $\text{RO}_2 + \text{RO}_2$ to dimer (R3c) compared to the other reaction channels (R3a,b) is higher for the more substituted aromatics. This is based on the assumption that the lamp produces similar concentrations of OH and HO_2 radicals and that the reaction rate coefficients $k(\text{RO}_2 + \text{HO}_2)$ (R4a) are similar for all RO_2 .

Line 127: You should clearly separate speculation, i.e., do you know if the stated radicals are forming observed dimers?

We agree, we replaced the text with:

Furthermore, we assume that less oxygenated radicals, although not quantitatively detected by the CI-APi-TOF (Berndt et al., 2015; Hyttinen et al., 2015), will nevertheless participate in the dimer formation.

Lines 145 to 174: In talking about products which main difference is the amount of O-atoms, it seems a bit confusing that all of them have the same label "z". Could you think of any other way of representing them so that it would not seem they all have the same "z-amount" of O-atoms.

We consider “z” as a variable which can be any number while we focus on the hydrogen atom number. To make it more explicit we added:
Where z denotes any number of oxygen atoms,

Line 174: Does this formula mean that you found products with 4 and 6 H-atoms more than in the parent VOC?. How could you get to a product with 6 H-atoms more than in the parent structure?

Can you give an example how this could happen?

HOMs with 6 hydrogen atoms more were in general a very small fraction of the total detected HOMs signal (this is true for the dimers as well). As an example one could think that the first OH adds one hydrogen atom to the initial ArHC and the termination of the radical chain to an alcohol or hydroperoxy function adds a second hydrogen atom. If the remaining 2 double bonds are not cleaved within the radical chain propagation this mechanism can be repeated up to 3 times, each time adding 2 hydrogen atoms. This can indeed lead to HOMs with 6 hydrogen atoms more than the ArHC precursor. This was already described in lines 194-197.

Line 181: What do you mean by “lower than expected H-atom number”?

We mean less hydrogen atoms than the precursor. We write now:

Similarly, the compounds with an H-atom number lower than the ArHC precursor could have been formed by an H-abstraction from first generation products with formula $C_xH_yO_z$.

Line 192: What do you mean by “much less H-atoms than terpenes”?

We mean that the fragmentation could involve the elimination of a fragment that contains hydrogen atoms instead of CO alone.

HOMs with less C atoms than the parent molecule have also been previously described from terpene precursors via CO elimination (Rissanen et al., 2014, 2015). Here, the aromatics show mostly also a loss of H-atoms when fragmenting. This indicates that a methyl group can be lost after oxidation to an alkoxy radical as formaldehyde or a carbon fragment can be lost after ring cleavage.

Line 192: Methyl group is not generally considered a good leaving group. Could you add a brief explanation or a reference?

If an H-atom is abstracted from a methyl group an alkoxy radical can be formed, which can decompose with the loss of H_2CO . See corrected text above.

Line 194: The occurrence of multiple OH attacks seems somewhat obvious from the observed product compositions. However, the given OH concentration together with such a short residence time in the flow tube does not seem to allow much 2nd generation oxidation (and of course even less 3rd generation). I think this fact should be addressed in the text. Perhaps a chemical reaction simulation could help to get an idea of the needed RO₂ lifetimes and the OH + product reaction rates to justify the high amounts of products evident from figures. Actually, the figures seem to indicate way higher product concentrations than what was the used reagent concentration ($=[OH]$). For example, Figure 3 gives a concentration of $>3 \times 10^9 \text{ cm}^{-3}$ for a single product, even though the stated $[OH]$ was only $2 \times 10^8 \text{ cm}^{-3}$ which should equal to the maximum product concentration, right?

The reported OH radical concentration is an average value. Due to the fast reaction the OH radical concentration is much higher at the beginning of the flow tube. Initial OH levels are about $8.5 \times 10^{11} \text{ cm}^{-3}$ and rapidly drop off a few orders of magnitude. Up to 23% of the precursor gas reacts and therefore an OH attack on the first generation products can occur in such a short reaction time. We report the modeled OH radical concentration in the Appendix C.

Line 201: What do you mean by “conjugated radical in an allylic position”? This should be rewritten.

We rephrased the whole sentence, see reply to comment on line 229 below

Line 205: What do you mean by “This mechanism varies among the ArHC tested.”? How is the mechanism changing?

We delete this sentence. Variations in the mechanism are provided just thereafter in the text.

Line 211: A reference should be added for: “termination reactions of alkoxy radicals make double bonds”. Is that a possible reaction for alkoxy radicals?

The manuscript is not correctly cited. We say that when the radical chain is interrupted the molecule can still have double bonds which are reactive sites towards OH radical attack.

Line 229: Oxygen bridged bicyclic radicals were not discussed in the text.

This was shown in line 204 and Figure 6. We rephrased it as follows:

After addition of OH and loss of aromaticity an oxygen molecule can be added forming a peroxy radical. It has been established that the latter can cyclize producing a second stabilized allylic radical with an endocyclic O₂ bridge (Baltaretu et al., 2009; Birdsall and Elrod, 2011; Pan and Wang, 2014). On this oxygen bridged bicyclic radical further oxygen addition and cyclization might occur up to a peroxy radical with seven oxygen atoms (C₉H₁₃O₇), which is the species detected at relatively high intensity (3.5%).

Line 230: The oxygen addition to allylic positions was not really discussed in the text.

It is now mentioned, see above.

Line 236: There was no discussion about phenolic structures in the main text. As already stated above, the current conclusions would rather fit as a continuation of discussion and not as a “conclusions” chapter.

We agree with the referee, we move this part to the results and discussion section and rephrased it:

Recent studies (Nakao et al., 2011; Schwantes et al., 2017) suggest a mechanism where the initial step is the formation of the phenolic equivalent ArHC followed by additional oxidation steps yielding “polyphenolic” structures with high O:C ratio (up to 1.2). However literature data are showing varying yields for the conversion of arenes to phenols via the OH radical addition and H elimination. According to MCM 3.3.1 (Jenkin et al., 2003) benzene and toluene have quite high phenol yields (approximately 50 and 20 %, respectively) while mesitylene shows a rather small yield (4%). This fact should be reflected in the final HOMs yield with alkyl substituted ArHCs being less effective in yielding HOMs. However in our experiments we did not detect such a difference in the HOMs yields linked to phenol formation yields. A relevant fraction of the detected HOMs showed a hydrogen atom number higher than the precursor ArHC which cannot be explained with the presence of just polyphenolic compounds as oxidation products.

Line 245: Please rewrite sentence starting with “Furthermore..”.

We replaced it with:

Furthermore, the fact that the oxidation of ArHC can rapidly form HOMs of very low volatility makes ArHC a potential contributor to nucleation and early particle growth during nucleation episodes observed in urban areas.

Figure 1: Excimer.

We corrected eximer with excimer.

Figure 2: I wonder what was your calibration procedure for the mass spectrometer?

The HOMs quantification is based on the calibration factor for sulfuric acid ($6.5 \cdot 10^9 \text{ cm}^{-3}$) and the assumption that HOMs have the same ionization efficiency as sulfuric acid (Ehn et al., 2014; Kirkby et al., 2016). It is known that the ionization efficiency depends on the structure of the HOMs. Since the ionization efficiency might be <1 for some HOM structures, the reported concentrations here represent lower limits. No further characterization of the system CIMS - ArHC HOMs was pursued.

Figure 4 caption: What do you mean by “ethylbenzene does not follow this empirical observation”? What is the empirical observation, and how ethylbenzene does not follow it?

With empirical observation we want to indicate the fact that with the increase of the number of the substituents less HOMs species are needed to sum up to the 80% of the total HOMs signal. While this is true for the series benzene, toluene, xylene, mesitylene, ethylbenzene deviates from this trend. This text now reads:

However, this trend with the increase of the number of substituents is not met by ethylbenzene

Figure 5: This figure needs some improvement: How do you go from $\text{C}_9\text{H}_{13}\text{O}_3$ through alkoxy radical to $\text{C}_9\text{H}_{13}\text{O}_6$? Also, you say that yellow box contains even oxygen species, even though it has also odd oxygen species.

The scheme is a simplified representation of the HOMs formation for mesitylene. We made two changes to the Figure: 1) The alkoxy radical chain is now in a separate box and 2) we added $\text{C}_9\text{H}_{13}\text{O}_4$ to the alkoxy radicals. The arrow links now the odd-oxygen radical box with the alkoxy (even oxygen number) box, from which then the even-oxygen radicals can be produced. The formation of the alkoxy radical can occur from any odd-oxygen peroxy radical. For example $\text{C}_9\text{H}_{13}\text{O}_6$ can be formed via two pathways:



We replace line 490 with:

Radicals in the orange box are from the propagation of the initial OH attack with an odd number of oxygen atoms, radicals in the pink box are formed via an alkoxy intermediate step with an even number of oxygen atoms, while radicals in the purple box are products of a second OH addition.

Table A-1: You talk about species losing methyl groups in the text, but what explains the benzene products with less C-atoms than the parent?

In the text we explained how a methyl group can be oxidized and become a good leaving group (e.g. formaldehyde). This is not possible for benzene. However if the autoxidation leads to a ring opening step the resulting radicals can undergo carbon chain fragmentation yielding small fragments (e.g. carbon monoxide, glyoxal).

Minor Comments:

Line 35: I don't think CCN (anymore) exert an influence on pre-industrial times (i.e., be careful with the wording).

We agree and changed the wording to:

CCN can impact climate via their influence on cloud properties; this changes the radiation balance nowadays and did even more so in the pre-industrial period (Carslaw et al., 2013; Gordon et al., 2016).

Line 44: I guess it's really hard to prove that something does not happen, right? So I'm a bit wondering why so many references have been grouped to indicate that no HOMs were seen by studies that did not use the current methods able to detect the HOMs in the first place.

We rewrote this to read:

Despite the fact that ArHC·OH adducts under atmospheric conditions react with O₂ to yield peroxy radicals (Calvert et al., 2002; Glowacki et al., 2009; Suh et al., 2003) it is not known if ArHC oxidation also yields HOMs. No carbon balance could be reached so far and generally only about 50% of the carbon reacted was identified as products (Calvert et al., 2002). When aromaticity is lost by the OH addition non-aromatic double bonds are formed representing highly reactive products to more oxidants, which is a peculiar behavior not observed in other classes of VOC (Calvert et al., 2002).

Line 49: Multiple non-aromatic double bonds exists also in many terpenoid species, so it's wrong to argue that this is a property of aromatics alone.

Here we want to say that if ArHC loose their aromaticity products can also become reactive towards other oxidants like O₃ and NO₃ (Calvert et al., 2002). We now point this out in the previous answer.

Line 67: I think it could help the reader if you could provide a bit more details about OH generation. At least I cannot fully understand the method how it's described now. Do you have an injector or why is the coaxial geometry mentioned?

More information is now provided in Appendix C. We mention the coaxial geometry because coaxial is the geometry of the excimer lamp we used for this series of experiments.

Line 79: "acid-base reaction" – do you mean salt formation?

We mean the abstraction of an acidic H-atom from the HOM by NO₃⁻, see reaction R2.

Line 96: The stated "monomer" and "dimer" ranges overlap.

Yes, since we studied ArHc with increasing molar mass it is not possible to give an unequivocal range for monomers and dimers for all species.

Line 99: Which one is 14 Th – methyl or ethyl group. . . ?

An H-atom is replaced by a methyl group: Methyl (CH₃(15 Th) – H(1 Th)). In case of ethylbenzene a CH₂ group is added compared to toluene. We changed the sentence to:

....is shifted by differences of 14 Th (CH₂) each from benzene via toluene and xylene/ethylbenzene to mesitylene due to the additional substituent groups

Line 107: What "a mechanism for Van der Waals interactions.." means? Is there a "mechanism"?

We replaced this with:

Most of the higher n-mers are probably bonded by intermolecular interactions, similar to biogenic HOMs (Donahue et al., 2013).

Line 108: I don't understand why would you talk about 800 Th cluster as a particle while talking about mass spectrometric results? Could you explain the significance of adding this here?

We made this link because clusters of this size can already be detected by particle counters. Thus mass spectrometry and particle measurements start to overlap and mass spectrometry can help to identify which compounds are participating in NPF. We modified the sentence:

Clusters with m/z ≥ 800 Th might already be detected by particle counters with a mobility diameter d ≥ 1.5 nm

Line 121: I wonder if a "monocyclic dimer" is a correct term here, if you do not know if the ring is retained in the reaction or not. Maybe better to reword to state that it is a "dimer" that was generated by monocyclic ArHC.

We agree and replaced this with:

while dimers that were generated from monocyclic ArHC have on average

Line 125: What is an “auto-termination reaction”?

It is an intramolecular decomposition that leads to a non-radical organic species and an OH radical as an example. We assessed a similar question from referee #1, to now read:

Additionally, more oxygenated radicals have a higher probability to undergo a unimolecular termination compared to a radical-radical recombination ($\text{RO}_2\cdot + \text{RO}_2\cdot$ or $\text{RO}_2\cdot + \text{HO}_2\cdot$). More oxygen atoms imply more peroxy functional groups and therefore a higher probability of a hydrogen abstraction in geminal position of a peroxide group which results in an OH radical loss and a carbonyl group formation. Therefore, the fraction of dimer formation should decrease with higher oxygen content.

Line 125: Where is the comparison between unimolecular and bimolecular channels based on?

As explained before, more oxygen atoms in the HOM imply more peroxide functional groups which increases the probability of the unimolecular pathway. This decreases the fraction of dimers with increasing oxygen content.

Line 128: What is a “higher-order cluster”?

With higher-order cluster we indicate n-mers where the precursor monomeric structure appears 3 or more times. While in the text we refer to them as trimers, tetramers and pentamers when the monomer structure appears 3, 4 and 5 times, respectively, we want to clarify that if monomers and dimers are produced via radical unimolecular termination or the radical-radical reactions reported in the text (R3a-c and R4a,b) higher order clusters (trimers, tetramers, pentamers) are most likely resulting from the aggregation of these monomer and dimer HOMs via the establishment of van der Waals interactions.

Line 134: add -s to “pathway”.

We replaced this with:

The increasing number of methyl groups appears to influence the oxidation pathways and leads to less HOM products.

Line 150: Both products have same number of O-atoms (=z).

We corrected the chemical formulas.

Line 153: Rather odd number of H-atoms?

In case of an OH addition an O-atom is added followed by O_2 additions, which leads to an odd number of oxygen atoms (z_o). In case of an H-atom abstraction O_2 adds to the carbon radical and further autoxidation would then produce an even number of oxygen atoms (z_e).

Line 157: Is Hyttinen 2015 the right reference for this?

Yes, it is.

Line 162: I don't think Kirkby 2016 is generally a good reference for peroxy radical mechanisms as it seems to contain all the mechanistic aspects in its supplementary material.

We removed Kirkby 2016 as a reference here.

Line 166: Also reaction 4b forms RO radicals.

We replaced this with:

These alkoxy radicals (R3a, R4b) may isomerize to an alcohol by internal H-abstraction forming a carbon centered radical.

Line 167: Oxygen molecule.

We replaced atom with molecule.

Line 169: What do you mean by “discrepancy between the intensity of the peaks”?

We find a prevalence of monomers with formulae $C_xH_{y+2}O_z$ compared to those with formulae $C_xH_yO_z$. On average reaction R3b should yield similar concentrations. From the flow tube kinetic model in Appendix C we note that the HO_2 radical concentration is very high during the whole experiment because it is also formed in the source. From this we infer that the radical termination reaction R4a is the main sink of the peroxyradicals under these specific conditions of our experiments .

We say now:

The much higher intensity of the peaks with formula $C_xH_{y+2}O_z$ compared to those with the composition $C_xH_yO_z$ can be ascribed to a high contribution from the recombination of $RO_2\cdot$ with $HO_2\cdot$ (R4a). This is due to the high HO_2 concentration in our experiments since HO_2 is also formed in the OH radical source.

Line 196: For which compounds the third OH attack is seen?

Benzene, ethylbenzene, xylene, naphthalene and biphenyl show HOMs that can be linked to a third OH attack. The contribution of these HOMs to the total of the detected signals is however always extremely low.

A third OH attack is observed only for some compounds: benzene, ethylbenzene, xylene, naphthalene and biphenyl; the contribution of these HOMs to the total of the detected signals is always extremely low. The mechanism will likely proceed in a similar way.

Line 211: Should be Kurten 2015?

The referee is right, we wanted to refer here to: Kurtén, T., Rissanen, M. P., Mackeprang, K., Thornton, J. A., Hyttinen, N., Jørgensen, S., Ehn, M. and Kjaergaard, H. G.: Computational study of hydrogen shifts and ring-opening mechanisms in α -pinene ozonolysis products, J. Phys. Chem. A, 119(46), 11366–11375, doi:10.1021/acs.jpca.5b08948, 2015.

Line 218: Too less C atoms in biphenyl dimer.

This was indeed a typo. We replaced with:

$C_{24}H_{22}O_8$.

Line 219: Aromatic rings are generally considered rather unreactive than reactive.

We wanted to say that the remaining aromatic ring is still quite reactive towards a second attack by OH radicals. We now say:

Compounds with extra-high H-atoms are more frequently found for biphenyl, which is expected as there is a second reactive aromatic ring remaining after (auto)-oxidation of the first one.

Line 234: Should be “and” not “or”.

We agree and changed this to and.

Line 467: Should be “due” not “doe”.

done

Table 1 caption: Why do you state “mixing ratio” here?

We replaced it with concentration.

Table 2: Would it make more sense to express the fraction in percentage so that the O:C and the fractional part would not be mixed so easily?

Good suggestion. We express now monomer and dimer fractions in percentage.

Figure 3 caption: There are no compositions in the given inserts, although they're mentioned. Can the mass spec really retrieve accurate compositions for the pentamers?

This class of mass spectrometer shows a resolution of 4-5000 with a flattening above mass 150-200 Th. Such resolution is certainly insufficient alone when it comes to provide a peak chemical composition at high masses. However, during the peak analysis process it is possible to infer the chemical composition of the peaks present in the mass spectra, taking advantage of the following assumptions:

- the elements possibly present are carbon, hydrogen; oxygen and nitrogen as a nitrate ion,
- the ratio between these elements has to allow a reasonable chemical structure (e.g. unsaturation number),
- the precursor carbon chain gives some constraints on the number of carbon atoms expected in the chemical formula with no fragmentation due to the ionization process because of the soft ionization method,
- the peak distribution can suggest a repetition of building blocks (e.g. monomer, dimer, trimer, tetramer) as well as peak compositions that differ by 2 hydrogen atoms (2.0157 amu) or 1 oxygen atom (15.9949 amu),

We do not report the chemical composition in the insert, however, all the peaks plotted here are identified with their chemical composition. Pentamers from biphenyl were identified up to mass 1242.3307 Th corresponding to the chemical formula $C_{60}H_{60}O_{25}(NO_3)^-$.

Line 242: I'm not sure if you should talk about identification here, rather "have curiously the same compositions as..". In addition I think also this part should be in Discussion section.

We agree. We now close the manuscript with a paragraph "Discussion and atmospheric implications" and we replaced the text with:

Some of the HOMs measured here from the oxidation of ArHC have the same composition as the HOMs formulae identified by Bianchi et al. (2016) during winter time nucleation episodes at the Jungfraujoch High Altitude Research Station.

Appendix B: Figures of the parent compounds also here would make the figures more interesting.

We included the ArHC structures in each figure.

1.92: If you present molar yields, you must have information about the sensitivity of your mass spectrometer. In addition the y-axis in Figures 2 and 3 seem to be given in molecule concentration. (If not, that should be clarified in the captions.) At C1 other parts of the manuscript you mention that you cannot quantify dimers because the transmission of your TOF-MS is unknown. In this manuscript, any information about the sensitivity of your instrument is missing. How did you estimate the molar yields then? Please, state precisely in the experimental section, what you did to determine the sensitivity or what the basis of your assumptions is.

We answered this point in our reply to referee #1. The HOM molar yield was calculated from the ratio of HOM concentration to reacted ArHC (the yields were not corrected for HOMs losses in the flow tube). The amount of ArHC reacted was calculated based on the assumption that the OH production was similar in all experiments. The OH concentration was determined from the difference in precursor concentration between excimer lamp switched on or off from two D9-butanol, toluene, mesitylene, and biphenyl experiments. The HOMs quantification is based on the calibration factor for sulfuric acid and the assumption that HOMs have the same ionization efficiency as sulfuric acid (Ehn et al., 2014; Kirkby et al., 2016). It is known that the ionization efficiency depends on the structure of the HOMs. Since the ionization efficiency might be <1 for some HOM structures, the reported concentrations here represent lower limits. No further characterization of the system CIMS - ArHC HOMs was pursued. We added the following in the text:

HOMs yields are calculated as the ratio of HOMs measured to ArHC reacted. HOMs were quantified using the calibration factor for sulfuric acid and assuming the same charging efficiency for HOMs (Ehn et al., 2014; Kirkby et al., 2016). From the decrease of the precursor concentration (lights off versus lights on) we determined an average OH concentration. From the experiments with D9-butanol, toluene, mesitylene and biphenyl an average OH concentration of $2 \cdot 10^8 \text{ OH cm}^{-3}$ was obtained. Assuming the same OH production of the lamp in all experiments ArHC reacted was calculated from the OH radical exposure using the reaction rate coefficients at 25°C.

Table 1 was complemented with HOMs concentration, reacted fraction of ArHCs and HOMs yield and looks now like this:

Table 1

Initial concentrations of precursors, reaction rate coefficients, ArHC reacted fraction (%), total HOMs concentration and HOMs yield (%) relative to the reacted ArHC. The mixing ratio of precursors was determined at the exit of the flow tube when the excimer lamp (OH generation) was switched off.

Compound	Concentration (molecules cm ⁻³)	k_{OH} ($10^{-12} \text{ cm}^3 \text{ molecules}^{-1} \text{ s}^{-1}$)	Reacted fraction (%)	[HOM] (molecules cm ⁻³)	HOMs yield (%)
Benzene (C ₆ H ₆)	$9.85 \cdot 10^{13}$	1.22	0.5	$1.2 \cdot 10^9$	0.2
Toluene (C ₇ H ₈)	$1.97 \cdot 10^{13}$	5.63	2.3	$4.4 \cdot 10^8$	0.1
Ethylbenzene (C ₈ H ₁₀)	$1.13 \cdot 10^{13}$	7.0	2.8	$9.4 \cdot 10^8$	0.3
(o/m/p)-xylene (C ₈ H ₁₀)	$2.95 \cdot 10^{12}$	13.6/23.1/14.3	//	$2.8 \cdot 10^9$	//
Mesitylene (C ₉ H ₁₂)	$2.46 \cdot 10^{12}$	56.7	22.7	$3.1 \cdot 10^9$	0.6

Naphthalene (C ₁₀ H ₈)	2.95 10 ¹³	23.0	9.2	1.4 10 ¹⁰	0.5
Biphenyl (C ₁₂ H ₁₀)	4.43 10 ¹³	7.1	2.8	1.8 10 ¹⁰	1.4

Reference for the *k*-rates: (Atkinson and Arey, 2003)

p4, l.119: Does the split off of O₂ explain the lower oxidation degrees of dimers assuming RO₂+RO₂ = ROOR +O₂ or not?

We think this could be an explanation. We already give this explanation in line 122ff. To corroborate it we would need dedicated experiments which are beyond the scope of this paper.

p.4, l.119f and p.6, l.162: I would propose to give here Mentel et al. 2015 somewhat more recognition as they described, based on experimental observations in context of autoxidation, this type of dimer formation including mixed dimers a year before Kirkby et al. 2016. The same is true for the alkoxy path.

We added Mentel et al., (2015) instead of Kirkby et al. (2016) in the citations given in line 124 and line 162.

p.4, l.192ff: “Additionally, more oxygenated radicals have a higher probability to undergo an auto-termination radical reaction compared to a radical-radical recombination (RO₂· + RO₂· or RO₂· + HO₂·).” I don’t exactly what you want to say with this statement in context of degree of methylation and dimer fraction. Less methylated aromatic compounds tend to more auto-termination? What means auto-termination - termination by internal reaction?

The referee seems to address our statement in line 124. Similar questions were also raised by referee #2. We report here our answer.

This statement can be derived from Rissanen 2014: We rewrote it:

Additionally, more oxygenated radicals have a higher probability to undergo a unimolecular termination compared to a radical-radical recombination (RO₂· + RO₂· or RO₂· + HO₂·. More oxygen atoms imply more peroxy functional groups and therefore a higher probability of a hydrogen abstraction in geminal position of a peroxide group which results in an OH radical loss and a carbonyl group formation. Therefore, the fraction of dimer formation should decrease with higher oxygen content.

p.8, l231ff: I think, that one should differentiate clearer between autoxidation by H-shift to peroxy radicals on one hand and by attack of the peroxy moiety to internal double bonds on the other hand. Although both reactions are internal rearrangements they are still of different character, as the first needs “mobile” H-atoms and the latter double bonds with potential to allyl radical formation. As a consequence the HOM formation in aromatic systems would be based - at least in parts- on a different mechanism?!

We agree with the referee. We rewrote this to read:

The autoxidation radical chain reaction is thought to proceed via intra-molecular abstraction of a hydrogen atom from an acidic C-H bond by a peroxy radical and the consequent formation of a hydroperoxy functional group and a carbon centered radical that can take up an oxygen molecule from the surrounding and eventually repeat the whole process *n* times (here called Type I autoxidation). In the case of aromatic compounds, when the aromaticity is destroyed, Type II autoxidation may happen by further addition of oxygen to the allylic resonance-stabilized radical followed by an attack of the peroxy group to the internal double bonds forming an oxygen bridge.

This can proceed up to a peroxy radical of 7 oxygen. We speculate that Type II autoxidation might also occur in organic molecules with two double bonds like isoprene and limonene.

p.4, l.96 Thomson

Done

p.7, l.218; “strongest dimer is C₁₂H₁₄O₈ for benzene and C₁₂H₂₂O₈ for biphenyl, respectively”. I guess a typo, as C₁₂H₂₂O₈ cannot be a dimer resulting from biphenyl.

Yes this was a typo. We replaced it with C₂₄H₂₂O₈.

References

- Baltaretu, C. O., Lichtman, E. I., Hadler, A. B. and Elrod, M. J.: Primary atmospheric oxidation mechanism for toluene, *J. Phys. Chem. A*, 113(1), 221–230, doi:10.1021/jp806841t, 2009.
- Berndt, T., Richters, S., Kaethner, R., Voigtländer, J., Stratmann, F., Sipilä, M., Kulmala, M. and Herrmann, H.: Gas-phase ozonolysis of cycloalkenes: formation of highly oxidized RO₂ radicals and their reactions with NO, NO₂, SO₂ and other RO₂ radicals, *J. Phys. Chem. A*, (2), 150923134432004, doi:10.1021/acs.jpca.5b07295, 2015.
- Bianchi, F., Trostl, J., Junninen, H., Frege, C., Henne, S., Hoyle, C. R., Molteni, U., Herrmann, E., Adamov, A., Bukowiecki, N., Chen, X., Duplissy, J., Gysel, M., Hutterli, M., Kangasluoma, J., Kontkanen, J., Kurten, A., Manninen, H. E., Munch, S., Perakyla, O., Petaja, T., Rondo, L., Williamson, C., Weingartner, E., Curtius, J., Worsnop, D. R., Kulmala, M., Dommen, J. and Baltensperger, U.: New particle formation in the free troposphere: A question of chemistry and timing, *Science*, 352(6289), 1109–1112, doi:10.1126/science.aad5456, 2016.
- Birdsall, A. W. and Elrod, M. J.: Comprehensive NO-dependent study of the products of the oxidation of atmospherically relevant aromatic compounds, *J. Phys. Chem. A*, 115(21), 5397–5407, doi:10.1021/jp2010327, 2011.
- Calvert, J. G., Atkinson, R., Becker, K. H., Kamens, R. M., Seinfeld, J. H., Wallington, T. H. and Yarwood, G.: The mechanisms of atmospheric oxidation of the aromatic hydrocarbons, Oxford University Press., 2002.
- Carslaw, K. S., Lee, L. a, Reddington, C. L., Pringle, K. J., Rap, A., Forster, P. M., Mann, G. W., Spracklen, D. V, Woodhouse, M. T., Regayre, L. a and Pierce, J. R.: Large contribution of natural aerosols to uncertainty in indirect forcing, *Nature*, 503(7474), 67–71, doi:10.1038/nature12674, 2013.
- Donahue, N. M., Ortega, I. K., Chuang, W., Riipinen, I., Riccobono, F., Schobesberger, S., Dommen, J., Baltensperger, U., Kulmala, M., Worsnop, D. R. and Vehkamäki, H.: How do organic vapors contribute to new-particle formation?, *Faraday Discuss.*, 165, 91, doi:10.1039/c3fd00046j, 2013.
- Ehn, M., Thornton, J. a., Kleist, E., Sipilä, M., Junninen, H., Pullinen, I., Springer, M., Rubach, F., Tillmann, R., Lee, B., Lopez-Hilfiker, F., Andres, S., Acir, I.-H., Rissanen, M., Jokinen, T., Schobesberger, S., Kangasluoma, J., Kontkanen, J., Nieminen, T., Kurtén, T., Nielsen, L. B., Jørgensen, S., Kjaergaard, H. G., Canagaratna, M., Maso, M. D., Berndt, T., Petäjä, T., Wahner, A., Kerminen, V.-M., Kulmala, M., Worsnop, D. R., Wildt, J. and Mentel, T. F.: A large source of low-volatility secondary organic aerosol, *Nature*, 506(7489), 476–479, doi:10.1038/nature13032, 2014.
- Glowacki, D. R., Wang, L. and Pilling, M. J.: Evidence of formation of bicyclic species in the early stages of atmospheric benzene oxidation, *J. Phys. Chem. A*, 113(18), 5385–5396, doi:10.1021/jp9001466, 2009.
- Gordon, H., Sengupta, K., Rap, A., Duplissy, J., Frege, C., Williamson, C., Heinritzi, M., Simon, M., Yan, C., Almeida, J., Tröstl, J., Nieminen, T., Ortega, I. K., Wagner, R., Dunne, E. M., Adamov, A., Amorim, A., Bernhammer, A.-K., Bianchi, F., Breitenlechner, M., Brilke, S., Chen, X., Craven, J. S., Dias, A., Ehrhart, S., Fischer, L., Flagan, R. C., Franchin, A., Fuchs, C., Guida, R., Hakala, J., Hoyle, C. R., Jokinen, T., Junninen, H., Kangasluoma, J., Kim, J., Kirkby, J., Krapf, M., Kürten, A., Laaksonen, A., Lehtipalo, K., Makhmutov, V., Mathot, S., Molteni, U., Monks, S. A., Onnela, A., Peräkylä, O., Piel, F., Petäjä, T., Praplan, A. P., Pringle, K. J., Richards, N. A. D., Rissanen, M. P.,

Rondo, L., Sarnela, N., Schobesberger, S., Scott, C. E., Seinfeld, J. H., Sharma, S., Sipilä, M., Steiner, G., Stozhkov, Y., Stratmann, F., Tomé, A., Virtanen, A., Vogel, A. L., Wagner, A. C., Wagner, P. E., Weingartner, E., Wimmer, D., Winkler, P. M., Ye, P., Zhang, X., Hansel, A., Dommen, J., Donahue, N. M., Worsnop, D. R., Baltensperger, U., Kulmala, M., Curtius, J. and Carslaw, K. S.: Reduced anthropogenic aerosol radiative forcing caused by biogenic new particle formation, *Proc. Natl. Acad. USA*, 201602360, doi:10.1073/pnas.1602360113, 2016.

Hyttinen, N., Kupiainen-Määttä, O., Rissanen, M. P., Muuronen, M., Ehn, M. and Kurtén, T.: Modeling the charging of highly oxidized cyclohexene ozonolysis products using nitrate-based chemical ionization, *J. Phys. Chem. A*, 119(24), 6339–6345, doi:10.1021/acs.jpca.5b01818, 2015.

Jenkin, M. E., Saunders, S. M., Wagner, V. and Pilling, M. J.: Protocol for the development of the Master Chemical Mechanism, MCM v3 (Part B): tropospheric degradation of aromatic volatile organic compounds, *Atmos. Chem. Phys.*, 3(1), 181–193, doi:10.5194/acp-3-181-2003, 2003.

Jokinen, T., Sipilä, M., Junninen, H., Ehn, M., Lönn, G., Hakala, J., Petäjä, T., Mauldin, R. L., Kulmala, M. and Worsnop, D. R.: Atmospheric sulphuric acid and neutral cluster measurements using CI-API-TOF, *Atmos. Chem. Phys.*, 12(9), 4117–4125, doi:10.5194/acp-12-4117-2012, 2012.

Kirkby, J., Duplissy, J., Sengupta, K., Frege, C., Gordon, H., Williamson, C., Heinritzi, M., Simon, M., Yan, C., Almeida, J., Tröstl, J., Nieminen, T., Ortega, I. K., Wagner, R., Adamov, A., Amorim, A., Bernhammer, A.-K., Bianchi, F., Breitenlechner, M., Brilke, S., Chen, X., Craven, J., Dias, A., Ehrhart, S., Flagan, R. C., Franchin, A., Fuchs, C., Guida, R., Hakala, J., Hoyle, C. R., Jokinen, T., Junninen, H., Kangasluoma, J., Kim, J., Krapf, M., Kürten, A., Laaksonen, A., Lehtipalo, K., Makhmutov, V., Mathot, S., Molteni, U., Onnela, A., Peräkylä, O., Piel, F., Petäjä, T., Praplan, A. P., Pringle, K., Rap, A., Richards, N. A. D., Riipinen, I., Rissanen, M. P., Rondo, L., Sarnela, N., Schobesberger, S., Scott, C. E., Seinfeld, J. H., Sipilä, M., Steiner, G., Stozhkov, Y., Stratmann, F., Tomé, A., Virtanen, A., Vogel, A. L., Wagner, A. C., Wagner, P. E., Weingartner, E., Wimmer, D., Winkler, P. M., Ye, P., Zhang, X., Hansel, A., Dommen, J., Donahue, N. M., Worsnop, D. R., Baltensperger, U., Kulmala, M., Carslaw, K. S. and Curtius, J.: Ion-induced nucleation of pure biogenic particles, *Nature*, 533(7604), 521–526, doi:10.1038/nature17953, 2016.

Kürten, a., Rondo, L., Ehrhart, S. and Curtius, J.: Performance of a corona ion source for measurement of sulfuric acid by chemical ionization mass spectrometry, *Atmos. Meas. Tech.*, 4, 437–443, doi:10.5194/amt-4-437-2011, 2011.

Lee, B. H., Mohr, C., Lopez-Hilfiker, F. D., Lutz, A., Hallquist, M., Lee, L., Romer, P., Cohen, R. C., Iyer, S., Kurtén, T., Hu, W., Day, D. A., Campuzano-Jost, P., Jimenez, J. L., Xu, L., Ng, N. L., Guo, H., Weber, R. J., Wild, R. J., Brown, S. S., Koss, A., de Gouw, J., Olson, K., Goldstein, A. H., Seco, R., Kim, S., McAvey, K., Shepson, P. B., Starn, T., Baumann, K., Edgerton, E. S., Liu, J., Shilling, J. E., Miller, D. O., Brune, W., Schobesberger, S., D'Ambro, E. L. and Thornton, J. A.: Highly functionalized organic nitrates in the southeast United States: Contribution to secondary organic aerosol and reactive nitrogen budgets, *Proc. Natl. Acad. USA*, 113(6), 1516–1521, doi:10.1073/pnas.1508108113, 2016.

Mentel, T. F., Springer, M., Ehn, M., Kleist, E., Pullinen, I., Kurtén, T., Rissanen, M., Wahner, A. and Wildt, J.: Formation of highly oxidized multifunctional compounds: autoxidation of peroxy radicals formed in the ozonolysis of alkenes – deduced from structure–product relationships, *Atmos. Chem. Phys.*, 15(12), 6745–6765, doi:10.5194/acp-15-6745-2015, 2015.

Nakao, S., Clark, C., Tang, P., Sato, K. and Cocker, D.: Secondary organic aerosol formation from phenolic compounds in the absence of NO_x, *Atmos. Chem. Phys.*, 11(20), 10649–10660,

doi:10.5194/acp-11-10649-2011, 2011.

Pan, S. and Wang, L.: Atmospheric oxidation mechanism of m-Xylene initiated by OH radical, *J. Phys. Chem. A*, 118(45), 10778–10787, doi:10.1021/jp506815v, 2014.

Rissanen, M. P., Kurtén, T., Sipilä, M., Thornton, J. A., Kangasluoma, J., Sarnela, N., Junninen, H., Jørgensen, S., Schallhart, S., Kajos, M. K., Taipale, R., Springer, M., Mentel, T. F., Ruuskanen, T., Petäjä, T., Worsnop, D. R., Kjaergaard, H. G. and Ehn, M.: The formation of highly oxidized multifunctional products in the ozonolysis of cyclohexene, *J. Am. Chem. Soc.*, 136(44), 15596–15606, doi:10.1021/ja507146s, 2014.

Rissanen, M. P., Kurtén, T., Sipilä, M., Thornton, J. a., Kausiala, O., Garmash, O., Kjaergaard, H. G., Petäjä, T., Worsnop, D. R., Ehn, M. and Kulmala, M.: Effects of chemical complexity on the autoxidation mechanisms of endocyclic alkene ozonolysis products: from methylcyclohexenes toward understanding α -pinene, *J. Phys. Chem. A*, 119(19), 4633–4650, doi:10.1021/jp510966g, 2015.

Schwantes, R. H., Schilling, K. A., McVay, R. C., Lignell, H., Coggon, M. M., Zhang, X., Wennberg, P. O. and Seinfeld, J. H.: Formation of highly oxygenated low-volatility products from cresol oxidation, *Atmos. Chem. Phys.*, 17(5), 3453–3474, doi:10.5194/acp-17-3453-2017, 2017.

Suh, I., Zhang, R., Molina, L. T. and Molina, M. J.: Oxidation mechanism of aromatic peroxy and bicyclic radicals from OH–toluene reactions, *J. Am. Chem. Soc.*, 125(41), 12655–12665, doi:10.1021/ja0350280, 2003.